THE USE OF MASS FORCES TO INCREASE THE EFFICIENCY OF JET PROPULSION

Thesis

by

Galen B. Schubauer

In Partial Fulfillment of the Requirements for the

Degree of Master of Science

California Institute of Technology

Pasadena, California.

1930

THE USE OF MASS FORCES TO INCREASE THE EFFICIENCY OF JET PROPULSION

Abstract

A scheme is suggested for increasing the efficiency of jet propulsion by combining the jet with an airfoil. The combination is called a jet-foil.

From a theoretical investigation of the jet when used in this respect, it is concluded that high propulsive efficiencies are possible under ideal conditions since the action depends upon mass forces and is completely independent of viscosity.

Experimental determination of the forces on four model jet-foils, made by measuring pressure distribution on the models when placed in a wind stream, showed an increase in lift of the model with the jet compared to that of the model alone, and an increase in drag for three of the models and a decrease for the fourth. The lift and drag depended upon the strength of the jet and upon the attitude of the model to the wind.

The efficiency of the jet-foil is defined as that fraction of the unused power of the jet which the jet-foil absorbs by doing work. Zero efficiencies are obtained for the three models showing increased drag, and values ranging from 38 per cent to zero for the fourth, which showed a decrease in drag. A second set of efficiencies were calculated neglecting increased drag. These range from 40 per cent to zero and are much the same for all of the models, decreasing as the strength of the jet increases. An effort is made to account for the low efficiencies on the basis of turbulence.

Contents

THE USE OF MASS FORCES TO INCREASE THE EFFICIENCY OF JET PROPULSION

I. Introduction

The reactive force produced by a jet of fluid may be utilized for propulsive purposes. In its simplest form of application the jet issues from a nozzle of circular orifice and the kinetic energy of the issuing fluid is extracted as useful work by the motion of the nozzle in the direction of the reactive force. The fluid after issuing mixes with the surrounding medium and the remaining kinetic energy is finally dissipated as heat and lost. It is obvious that the work done upon the nozzle and the object to which it is attached is a small fraction of the total energy expended if these have a speed which is a small fraction of the speed of the jet.

The question of using simple jets of hot gas for the propulsion of airplanes has been studied by Buckingham[1] with the conclusion that the propulsive efficiency is too low at the ordinary speeds of airplanes to make the scheme practical unless an additional propulsive force is obtained from the motion induced in the surrounding air. Buckingham states that attempts have been made to use guide rings about the jet, such as are used in aspirators and injectors. These rings fulfill the two-fold purpose of reducing frictional losses about the jet and giving rise to an additional reactive force. They accomplish both by deflecting air in the direction of the jet which is drawn towards the jet by reduced pressure.

The function of the rings illustrates two fundamental requirements for increasing propulsive efficiency. These are: first, an efficient transfer of kinetic energy from the jet to the outer medium; and second, the placing of this kinetic energy there in motion of such form that it shall produce additional reactive forces and so be extracted as work done upon the object being propelled. In this paper a different scheme is proposed for fulfilling these two requirements.

The method proposed has two outstanding features: first, a two-dimensional nozzle or one approximating the two-dimensional is moved transversely to the direction of propulsion and to its infinite dimension; and second, the orifice of the nozzle is placed along the under surface at the trailing edge of a modified type of airfoil. The first gives promise of securing an efficient transfer of energy by bringing into play inertial forces. The second aims at a very complete recovery of energy from the two-dimensional disturbance in the outside medium caused by the jet in its sidewise motion. Actually the two-dimensional condition can only be approximated by using a large aspect ratio, or shielding the ends of a small section.

To facilitate discussion, we shall understand the term transverse motion to mean sidewise motion only of the two-dimensional nozzle or jet, and the term simple jet to refer to the two-dimensional jet without transverse motion. The modified airfoil in combination with the nozzle will be called a jet-foil, and in certain cases where we refer to the experimental work the term model will carry the same meaning.

While the actual mechanism for employing this scheme of propulsion and the mechanical and thermodynamical problems involved are outside the scope of this paper, it may be suggested out of practical interest that an application of the jet to airplane propulsion might be made by replacing the airfoils of a screw propeller by jet-foils, and using one component of the total reactive force to rotate the propeller, while the other component is used to propel the airplane. Mention is made of this scheme because the problem first suggested itself in this light.

We shall first examine the proposed scheme on theoretical grounds. Following this, an effort will be made to show its value by presenting the results of experimental tests made on the four models shown in Fig. 6 .

II. Theory of the Two-Dimensional Jet

A theoretical treatment regarding the form of a two-dimensional jet and the process of energy transfer from it to the surrounding medium will be given for the two special cases where, first, the nozzel is stationary with respect to the undisturbed medium surrounding it, and, second, where the nozzle has a transverse motion only. In both cases the jet fluid and that of the exterior will be identical, incompressible, and viscous, except where an inviscid medium is used for comparison. Since in jet propulsion we are primarily interested in a gas, the theory will later be shown to apply here with only slight modifications for compressibility. Furthermore, the treatment will include all ranges of velocities.

1. The Jet Without Transverse Motion.

a. The difference between viscid and inviscid flow.

According to theory of classical hydrodynamics, the Eulerian flow or flow of least energy results when an inviscid fluid issues from a nozzle such as that shown by the heavy lines at $x = \pm\pi$ in Fig. 1. The stream-lines and equipotential lines of Eulerian flow in two dimensions, which are shown on an xy-plane in Fig. 1, are related to the xy-coordinates by the equations:

$$y = -\phi + e^{-\phi} \cos$$
$$x = -\psi - e^{-\phi} \sin$$

where the lines along which ϕ is constant are the equipotentials and those along which ψ is constant are the stream-lines.

According to Lanchester[2], Fig. 1 shows the field of force and mechanical potential which arises when an external

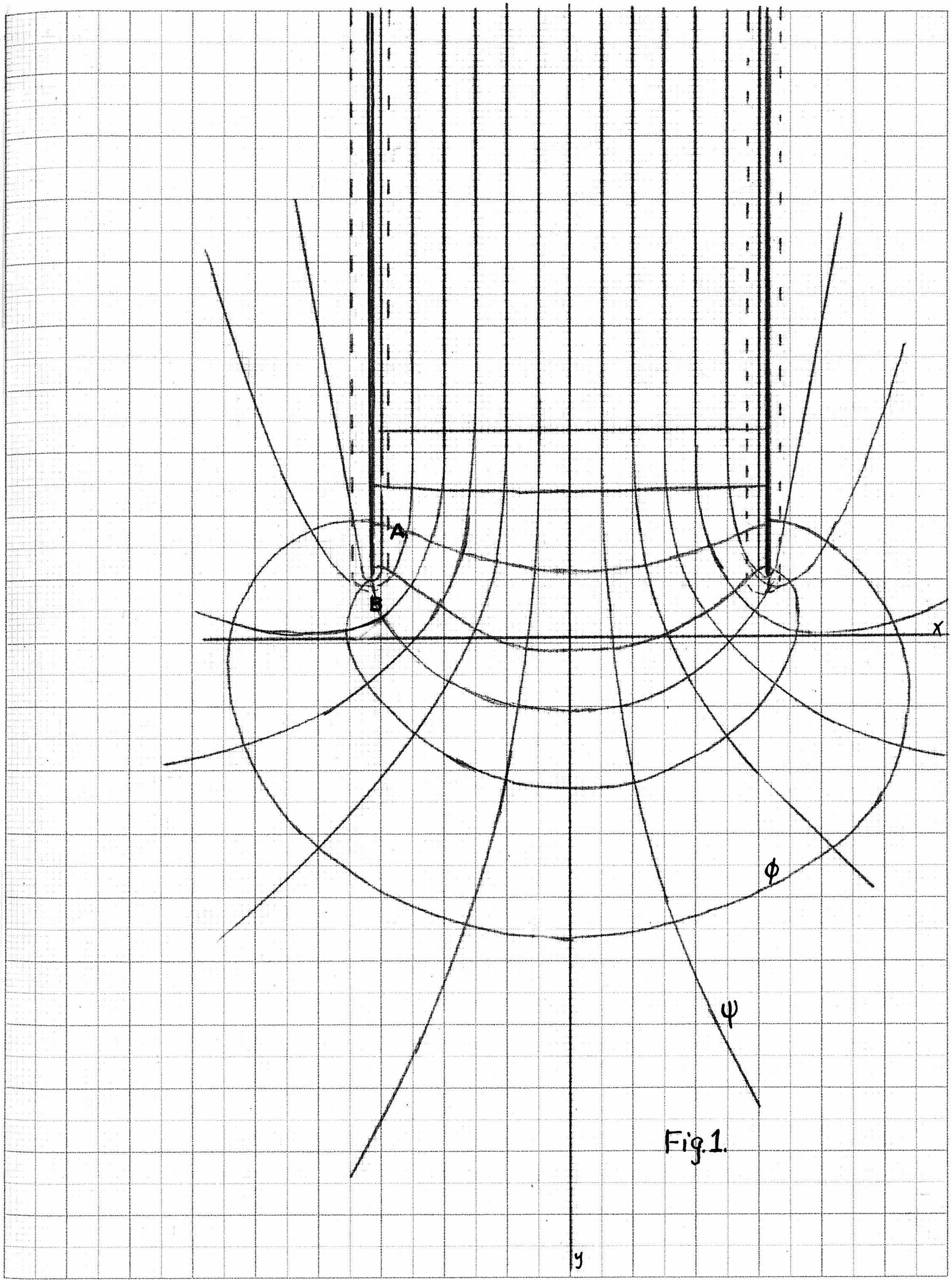

Fig.1.

force is applied to drive the fluid from the nozzle. The acceleration takes place along these lines of force, and the stream lines of both viscid and inviscid fluids initially follow them, except at points of infinite curvature on the boundary[3]. In a viscous fluid, and this is the one with which we are chiefly concerned, the condition of no slipping at the boundary alters the picture of the initial motion on the boundary, but not appreciably elsewhere until, as we shall presently see, changes in the viscous flow, which are well known to exist, have had time to take place. We shall now study these changes in detail.

The dotted lines in Fig. 1 show nozzle walls of finite width and rounded ends to eliminate points of infinite curvature. Outside of the very thin inert layer next to the boundary, the particles of fluid accelerate due to an applied force; and the lines of acceleration and initial flow near the boundary tend to follow its general contour. Inertial forces cause the pressure to decrease as we go along the boundary from a point A on the inside to some point B on the rounded end. The inert fluid next to the boundary tends to be carried along with the main flow from these regions of higher pressure to those of lower and will, as the result, accumulate on the rounded end where the pressure is a minimum[4]. A region of inert fluid has its origin here and continues to grow until it finally occupies the entire external region, except that directly below the orifice, unless the viscous forces between the inert and the moving fluid are large enough to drag the inert fluid out of these regions as fast as it tends to accumulate there. The greater the viscosity, the thicker is this boundary layer, and consequently the greater is the rate of departure from the Eulerian or potential type of flow. At the same time, viscosity by its dragging action tends to prevent the final departure from becoming complete[5].

Dorsey[6] in his study of efflux from capillary tubes describes the process of departure as follows: "When the flow is exceedingly slow, the colored liquid oozes out of the capillary and flows away in all directions, forming a slowly growing, nearly hemispherical cap, seated against the end of the tube. As the velocity is slowing increased this condition persists for a time; but presently while the velocity is still very low, the cap is seen to move bodily from the end of the tube, developing a stem".

Very definite evidence of the dragging action of viscosity was found by Smoluchowski[7] in his work with jets of water and glycerine issuing from a hole in a thin plate. Here it was found that the dragging action might be very complete; and in cases of low velocities and high viscosities, the stream-lines approximated the Eulerian type quite closely.

b. Boundary process about a jet of viscous fluid.

Generally then we may say that the jet is bounded by the inside planes of the nozzle walls produced, and the fluid in the remainder of the external space moves only as it is dragged along by viscous shearing stresses. This, however, is treating the flow as though it were laminar, which we know is not always the case.

At all velocities except very low ones, the jet is surrounded by a turbulent sheath made up of vortex filaments which follow each other in rapid succession. It is Lanchester's[8] view that these act as rollers between the layers of different velocity.

Using Prandtl's[9] theory of turbulence, Tollmien[10] has treated conditions at the jet boundary somewhat as follows: A portion of fluid is imagined to move normal to the jet because of collisions between the jet and the exterior medium. The motion of this body of fluid through a region where a velocity gradient exists gives rise to an eddy shearing stress, $\mathcal{T}$, with which Tollmien replaces pressure in the general Eulerian equation of motion and is thus enabled to calculate the distribution of velocity about the jet.

c. <u>Kinetic energy loss and efficiency.</u>

We may now estimate the energy losses in the light of these boundary processes. In the case of laminar flow the transfer of motion depends entirely upon the shearing stresses in the viscous fluid. Since we here require friction between contiguous layers, it follows as a corallary that no motion can be imparted to the exterior fluid by the jet without energy loss. When the motion is turbulent, on the other hand, we may use Prandtl's expression for $\mathcal{T}$ to examine the mechanism of transfer. Prandtl writes:

$$\tau = \rho \, l^2 \left| \frac{\partial \bar{u}}{\partial y} \right| \frac{\partial \bar{u}}{\partial y}$$

where ρ is the density, l is the mixing path, $\bar{u}$ is the mean velocity in the direction of the jet, and y is the coordinate normal to the jet. We see that τ, the pressure term, in Tollmien's equation of motion cannot exist without a velocity gradient and consequent energy loss.

Having considered the laminar and turbulent motions, we may draw the conclusion that energy loss must accompany these ordinary processes of energy transfer. In addition to what has been said, it may be added that as far as an application of the jet to propulsion is concerned the energy of motion of the vortices in turbulent flow is lost since this motion has no resultant linear momentum, and hence cannot give rise to a reactive force.

Kinetic energy loss may be treated in a different light by taking into account the conservation of linear momentum. If the condition be imposed that the induced motion shall have the same direction as the jet, as is required in Fig. 2, we find the momemtum equation to be

$$m_1 v_1 - m_1 v_t = M v_t - M v_s \tag{1}$$

where M = mass per second flowing in large stream

m_1 = mass per second issuing from the nozzle

v_1 = jet velocity

v_s = initial stream velocity

v_t = final uniform velocity where the jet has mixed with the stream

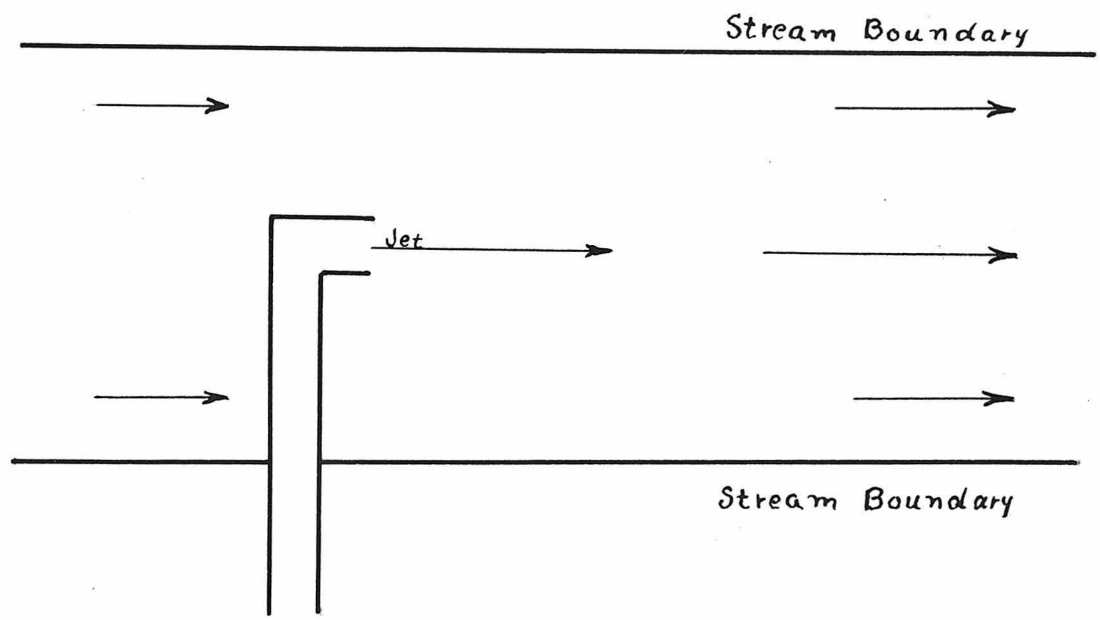

Fig. 2.

From equation (1) we have

$$v_t = \frac{m_1 v_1 + M\ v_s}{m_1 + M}$$

The power in the stream where the jet and stream have mixed and the velocity has become uniform is

$$E_t = 1/2\ (M + m_1) \left(\frac{m_1 v_1 + M\ v_s}{m_1 + M}\right)^2$$

The power added to the stream by the jet is

$$\Delta E = 1/2 \left[(m_1 + M) \left(\frac{m_1 v_1 + M\ v_s}{m_1 + M}\right)^2 - M\ v_s^2 \right]$$

If the efficiency η be defined as the ratio of the power added to the stream to the power of the jet, we may write

$$\eta = \frac{(M + m_1) \left(\frac{m_1 v_1 + M\ v_s}{m_1 + M}\right)^2 - M\ v_s^2}{m_1\ v_1^2} \tag{2}$$

The added efficiency obtained by giving the mass to be accelerated by the jet an initial velocity may be seen when v_s is set equal to zero in equation (2). The efficiency is reduced to

$$\eta_1 = \frac{m_1}{M + m_1} \tag{3}$$

Hence for high efficiency for the case where the final motion is required to have the initial direction of the jet the mass to be accelerated must be kept small or must have an intially high velocity.

If the induced motion has components normal to the initial direction of the jet as well as along it, conservation of momentum no longer requires an energy loss. In fact, the efficiency is increased from the minimum value just given in proportion to the amount of side motion arising. A pure potential flow, which under certain conditions may be very closely approximated in a viscous fluid, may accelerate an indefinitely large mass with only slight loss due to viscosity. It is because of the possibility of high efficiency in Eulerian flow that an attempt is made to obtain it by the transverse jet action, to be explained in a following section.

2. Imaginary Device for Maintaining Potential Flow

Looking again at the picture in its totality instead of its finer structure, we see the jet as a sheet of rapidly moving fluid literally slipping between two dead fluid regions, with friction dissipating the kinetic energy as heat at the boundaries. Knowing the type of initial flow to be quite different and of a spreading nature, one might ask why not annihilate the jet after its flow has changed to the linear type and cause it to reappear in undisturbed medium, continuing this process as long as we wish to maintain a type of flow similar to the inviscid? We shall show that this is in effect what is accomplished by moving the jet transversely.

3. The Transversely Moving Jet

It is now our purpose to use the jet theory previously given to determine the type of flow which will arise when a two-dimensional jet has been given a steady transverse motion through the exterior medium. In studying the processes we shall regard the fluid as incompressible and later show the modifications which result when the fluid is a gas.

For simplicity and to be consistent with the imaginary process of annihilation and reappearance of the jet, as previously described, we wish to keep the motion of the jet independent of any transverse motion of the nozzle, when the nozzle and the coordinate system of Fig. 3 move together with respect to the undisturbed medium. To do so, the type of nozzle shown in Fig. 3 is required. Here the nozzle walls CB and DE will be given an angle θ with respect to the X-axis such that for any velocity of the nozzle in the negative x-direction relative in magnitude to that of the jet, the jet will maintain its initial negative y-direction. The vectors a', b', and c' representing the jet velocity v_1 will be independent of any motion of the nozzle. Since for the present we wish to limit the disturbance of the jet to the medium in the third quadrant, and also to shield this portion of the medium from any nozzle disturbance, we shall add the plane AB across which no fluid is allowed to pass. We shall further limit ourselves to the surface of contact between the jet and the exterior, across which any disturbance must pass, and in particular to the origin of this surface at the corner, B. We shall select particles of exterior fluid such as a, b, and c below the plane AB

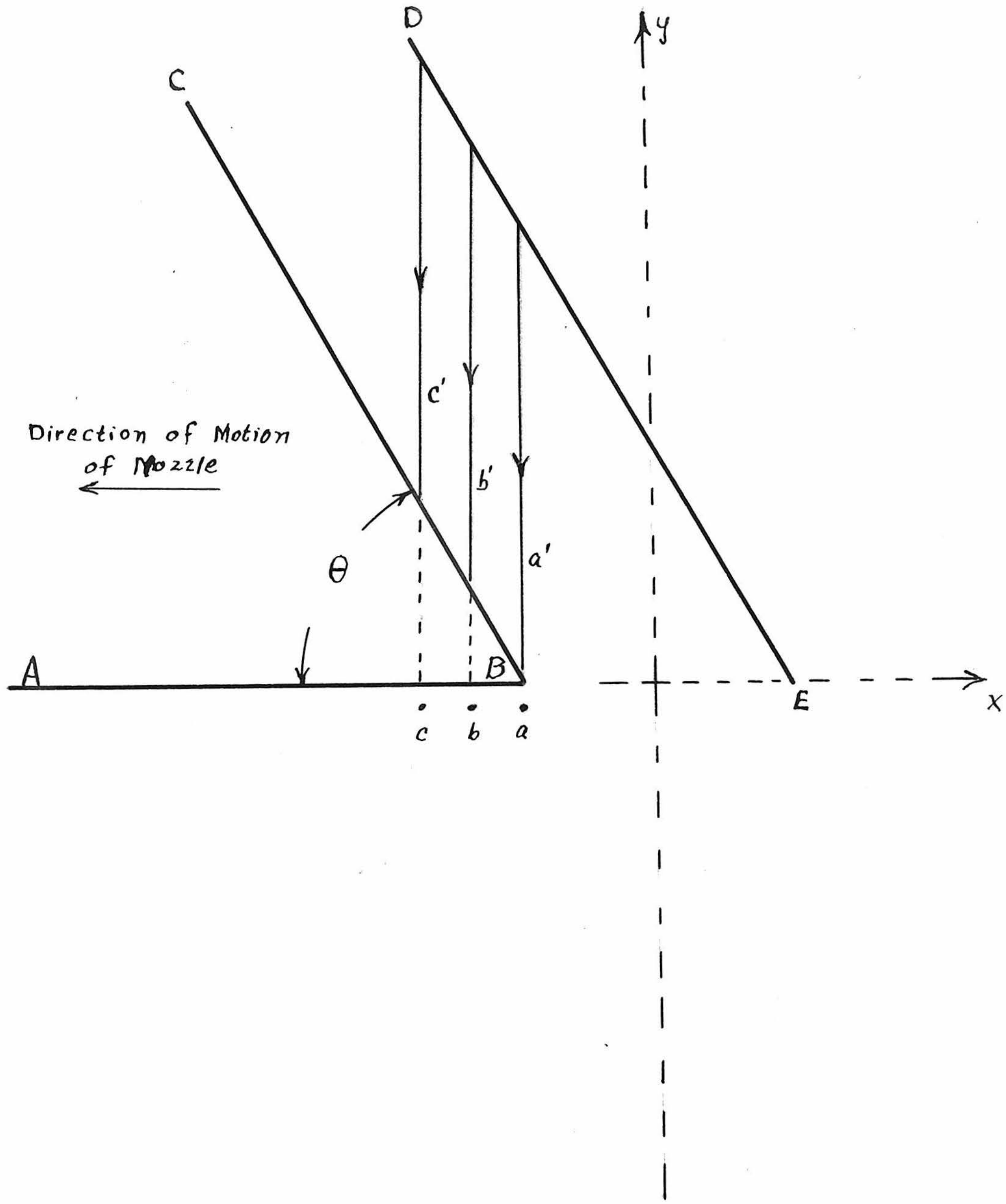

Fig. 3.

and just outside of the boundary layer of this plane, and shall study these as prospective contact points between the jet and the exterior.

It shall be understood at the start that the foregoing simplifying assumptions are in no way essential to transverse jet action. Later it will be shown that the jet influences the entire exterior region, and that it does so for a range of values of θ above and below that required in Fig. 3.

a. <u>Tracing of the physical processes.</u>

If it is assumed that during transverse motion the fluid below AB is not disturbed by the jet, which, as we have seen is approximately the case when the nozzle has no transverse motion, the particles in the fluid lines a', b', and c' will successively impinge upon the particles a, b, and c, as they are liberated at the point B. Since the medium is continuous, particle (a) and any line of particles such as a' are really small regions which are for convenience regarded as particles. The impact is then the result of a collision of one region with another, and in accordance with jet theory previously discussed the motion of (a) and the fluid surrounding it must begin as that of an inviscid fluid, but later depart in such a manner as to allow (a) and the particles below it in line with the impinging vector to move independently of the fluid on the side towards b, except for the dragging action of viscosity. However, immediately after (a) has been set in motion, the nozzle has moved and the adjacent particle to the left starts a similar cycle, and so the process continues.

The question of the resulting type of flow is clearly one of the rate of growth of the inert region and the rate at which the action of the jet is carried into this region to limit the time for the accumulation of inert fluid. As the condition of zero time of accumulation is approached, the flow must approximate more and more nearly the potential type. To avoid the academic question of flow about sharp edges, the corner at B may be regarded as slightly rounded.

The assumption that the medium below AB is undisturbed by the jet action is of course invalid since the action of the jet upon fluid previously under AB may have produced a disturbance which extends to this region, having the effect of moving the fluid from B to A . When the velocity of the jet with respect to the transverse motion is such that the impact pressure at the point of collision becomes equal to or greater than the dynamic pressure of the exterior medium (regarding as having the transverse motion), the fluid under AB will be driven ahead as fast as the nozzle moves, and any exterior particle such as (a) will be replaced by jet fluid which will then be subjected to the impinging action of the newly liberated jet particles such as those in the line a' . As far as transfer of motion is concerned, it makes no difference whether the jet acts upon its own fluid or that of the exterior, since the fluid replacing the exterior lies in contact with it and must eventually give over all of its motion to the exterior. We have endeavored by this type of treatment to show that the impinging action described in the previous paragraph is unaltered, except for the initial motion of the fluid acted upon by the jet, when the fluid under AB is driven ahead of the approaching jet.

We may apply the same reasoning when the jet has any direction except that parallel to the motion of the nozzle. Hence we see the arbitrariness of angle θ .

Since the first element may be seen in Fig. 4 to occupy successively all points of the orifice, we may conveniently study the whole of the jet by tracing any element as it advances with time through positions 1, 2, 3, 4, etc. The inert fluid has its origin at B and growing from there will reach these positions after successively longer time intervals. Obviously, then, there is some one of these positions for any ratio of jet velocity to transverse velocity to which the inert fluid can just reach and beyond which the flow must take place as though the fluid were inviscid.

In extending the effect of the jet to the medium in the first and fourth quadrants, we observe in Fig. 4 that the medium in the first quadrant will be drawn and that in the fourth will be driven in the negative y-direction. Going still further in Fig. 5, which shows the whole jet-foil of which Fig. 4 is a magnified view of only the rear portion, we find the motions already described to be part of a general circulation produced about the jet-foil by the jet.

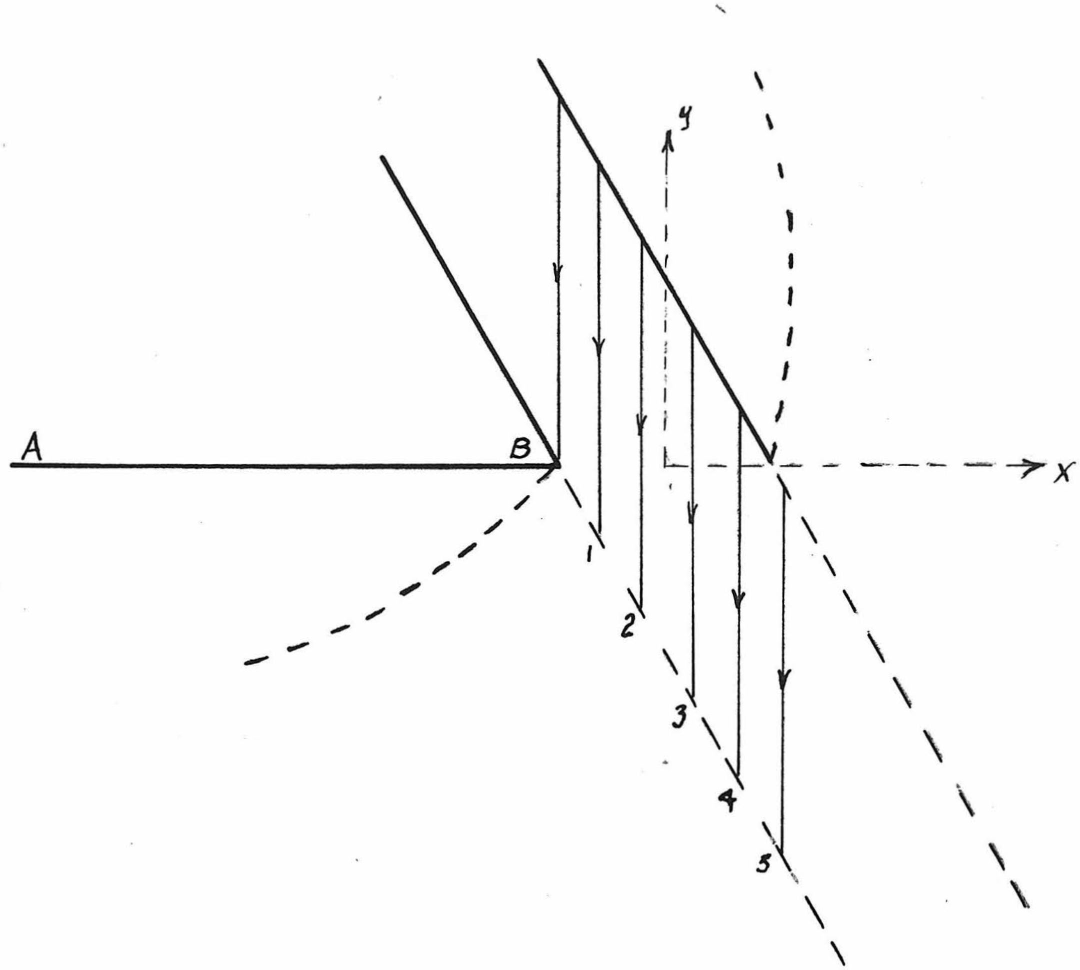
y
A
B
X
1
2
3
4
5

Fig.4.

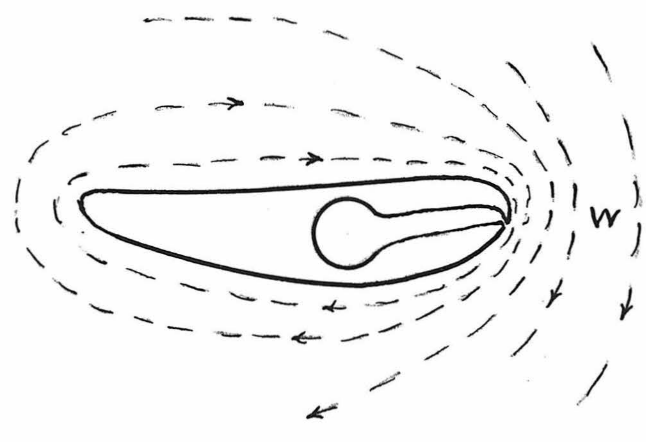
W
Circulation drawn to account for flow observed at W

Fig.5.

Fig. 5 is drawn to show conditions for Model No. 4 in an air stream as they were actually observed to exist by means of a fine silk thread. At W turbulence was always found to a degree depending upon the profile of the model and the strength of the jet. Without the jet the profile is poor aerodynamically, but with it the blunt trailing edge becomes permissible because of the large downward velocity of the medium in the rear.

b. Possible efficiency of the energy transfer.

We now have a picture of the way in which exterior motion originates. The transfer of kinetic energy depends entirely upon inertial forces brought into play by transverse motion and is entirely independent of viscosity. No energy loss is here required for the transfer of motion, as it is in the case of the simple jet discussed in the first part of the theory.

We have in addition means of estimating the overall efficiency of transfer from the detailed and general pictures given in Figures 4 and 5 respectively. The greater part of the motion corresponds closely to the ideal type of Fig. 5, in which viscosity forces are small compared to inertial forces. Here it is possible to transfer a large amount of kinetic energy with little friction loss. An inert region or jet wake will be assumed always to exist where the same losses will occur as at the boundary of the jet without transverse motion. In the present case, it is at least possible to make the wake small whereas in the absence of transverse motion it cannot be limited and extends to where the jet loses its identity. We shall be able to make a more accurate estimate of the efficiency when we see the function of the jet-foil.

c. The function of the jet-foil.

When a transverse motion is superposed upon the circulation shown in Fig. 5, the result will be a lifting force Fy. If the model is now allowed to move in the direction of Fy as well as transversely, in effect setting the model at a negative angle of attack, work will be done by the force, and the result is an absorption of the energy of circulation. Expressed in other terms, the jet-foil absorbs energy placed in the surrounding medium by the jet when by its motion it induces a circulation in opposition to that of the jet. Thus the total force, neglecting the drag of the model, has a component in the direction of motion of the jet-foil, and the work done is the product of this component by the velocity of the motion.

Most of the useful work done is transmitted from the original jet fluid through the potential region of the outer medium to some point on the jet-foil where it is absorbed, and the major portion of the losses probably occur between this moving potential region and regions of inert or eddying fluid. For high over-all efficiency, then, we must stress the elimination of turbulent wakes whether these be of the jet or of the jet-foil.

4. Application of the Theory to Air.

The general theory may be applied specifically without alteration to air at velocities below the acoustic where compressibility is not appreciable. At higher velocities the compressibility cannot be neglected; but in cases where the density is a function of pressure only, the general theory of physical processes about the jet remains valid.[11]

In a compressible medium, we find a standing shock wave diverging from the end of a nozzle from which a jet is issuing at or above the acoustic velocity[12]. An analysis of the origin of this wave will show that it can exist only outside or bordering a potential region. In the case of the transverse jet it is only when the jet-foil itself moves with the velocity of sound and so keeps pace with the advancing jet disturbance that the potential region will be limited and bordered by the shock wave.

It suffices merely to mention the wave-like impulses which accompany the impact of the jet with the inert fluid. These normally accompany the acceleration of any compressible fluid and are of academic rather than of practical interest.

III. Apparatus and Experimental Procedure

1. The Jet-Foils

Experimental tests made to determine the characteristics of jet-foils consisted of measuring forces on models with and without the jet when placed in a wind stream. The four models for which data are given are shown in Fig. 6.

EXPERIMENTAL JET—FOILS IN ACTUAL SIZE

No.1 Profile View

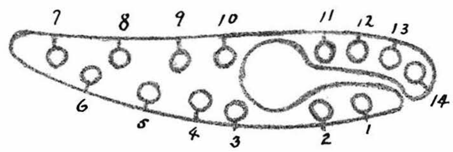

No.2. Profile View

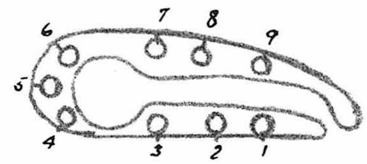

No.1 Bottom View

No2 Bottom View

No.3. Profile View

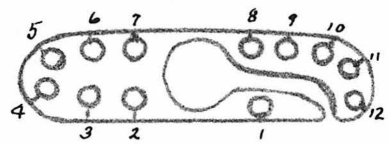

No.4. Profile View

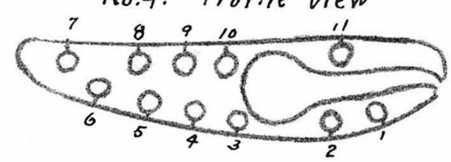

No.3. Bottom View

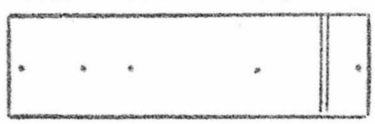

No.4. Bottom View

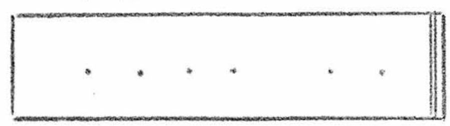

Göttingen 387 – F.B. Airfoil

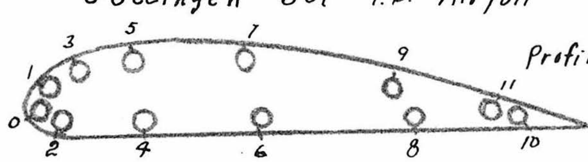

Profile

Numbers on periphery identify the pressupe orifrces

Bottom

Fig. 6

For making the tests it was desired to use models of easy construction since it was thought necessary to build a number of them varying the profile and nozzle location. The method finally adopted was to use models of one-half inch span (cut from one-half inch brass plate), shielding the ends with discs several times the size of the model, and then to determine forces on the model from the pressure distribution over the surface when an air stream was directed between the discs. A full size view of a model in the stream is shown in Fig. 7.

The models shown in Fig. 6 represent only a few of the total number built and tested. These four are the only ones which have the nozzles at the trailing edge. Those not shown have nozzles near the middle of the lower surface and proved to be so bad aerodynamically that the results of the tests are not given. The four shown for which results are given represent a variety of profiles from which it was hoped the optimum might be determined. These serve also to vary experimental conditions, e.g., degree of turbulence and degree of lift and drag with and without the jet. Since little was known of the reliability of this method of testing, a model air-foil with a Göttingen 387-F.B. profile upon which pressure distribution data are available[13] was included for comparing results obtained with this apparatus with those obtained in the conventional wind tunnel.

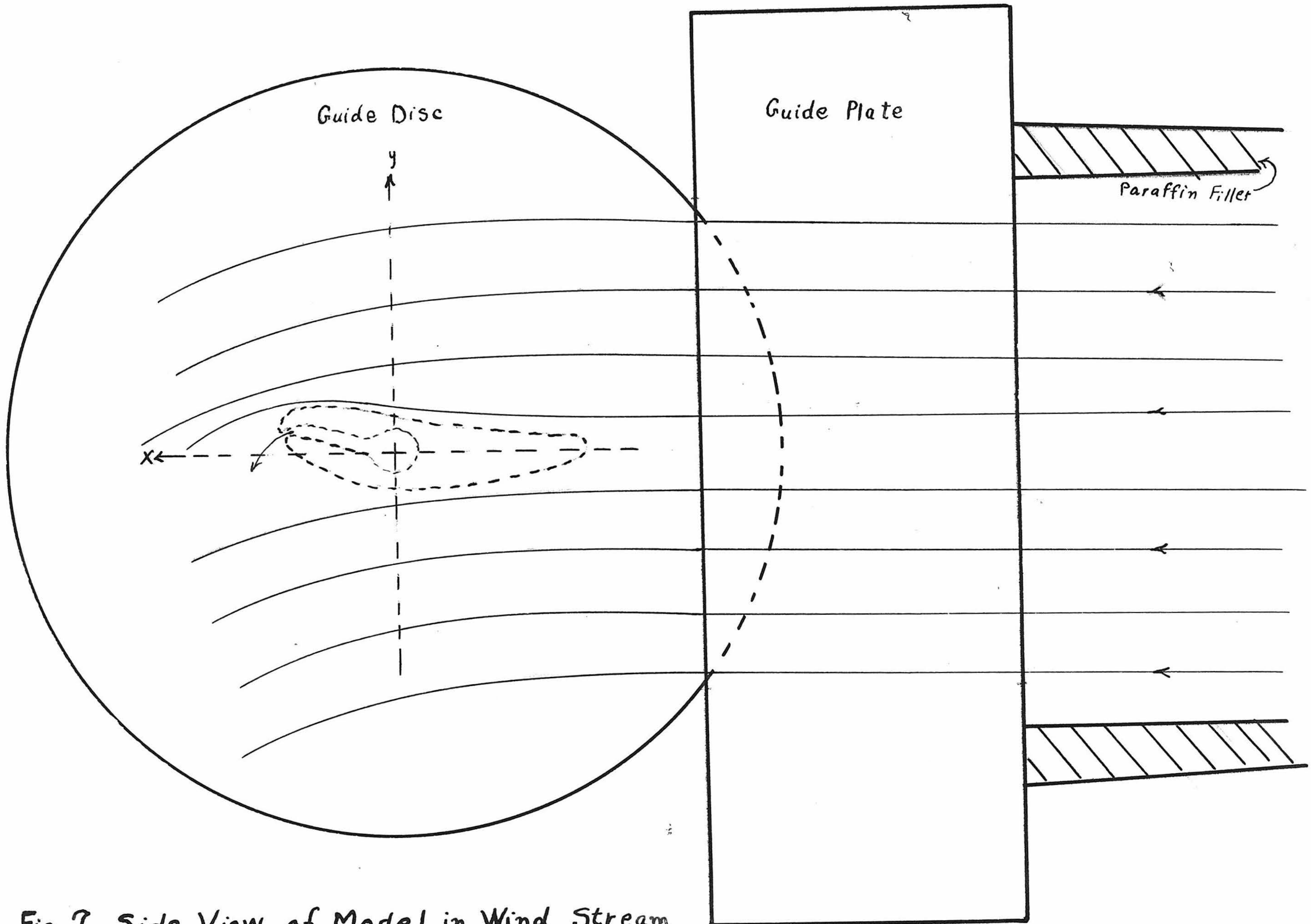

Fig. 7 Side View of Model in Wind Stream

The air for the jet is conducted into the model through a feed pipe fitting the central hole and from there to the nozzle through an air passage which may be seen in the four models in Fig. 6. The feed pipe extends through the model, one end being attached to the source, and the other being reduced to a pressure tap leading to a long mercury manometer. The pipe also serves as an axle upon which the assembled unit may be rotated. Eighth-inch holes were drilled around the outer edge of the section extending only half through the models to connect by copper tubes the 0.043-inch pressure orifices drilled normal to the surface. Because of the curvature of some parts of the surface, this size of orifice is the maximum permissible[14]. The copper tubes inserted into the holes around the periphery made possible the connection of the pressure orifices by rubber tubes running to the multiple manometer. The guide discs of two and three-quarter inch radius were soldered to the ends of the model when the pressure tubes and feed pipe were in place. The soldering served to seal the sides of the air passage and tube connectinns as well as to hold the discs firmly in place. The completed units are shown in Fig. 12. A few dimensions of the models are given in Table I.

TABLE I.

Dimensions of Models

	Dimensions in Inches			
	No.1	No.2	No.3	No.4
Chord	2.24	1.75	1.90	2.24
Maximum height above chord line	0.53	0.57	0.46	0.53
Width off nozzle orifice	0.031	0.050	0.031	0.025

2. General Description of Apparatus

The wind stream in which tests were made was obtained from a large compressed air main in the Daniel Guggenheim Aeronautics Laboratory. The same source supplied the air for the jet. Fig. 8a shows the general arrangement for expanding the air from the main to a four-inch by one-half inch stream directed between the guide discs on the models. Fig. 8b is a top view of the air passage, showing the expanding tube, the rectangular guide plates, and the model with shielding discs at A, D, and E respectively. Fig. 9 is a side view of the same, showing how the models are held in place. A small petot tube is inserted through one of the rectangular guide plates at F (Fig. 8b) for measuring wind velocity.

Figures 9, 10, and 11 show the method of connecting the pressure orifices to the multiple alcohol manometer by which pressure distributions and wind speed were measured. In Fig. 10 the fluid meter is shown at G , the

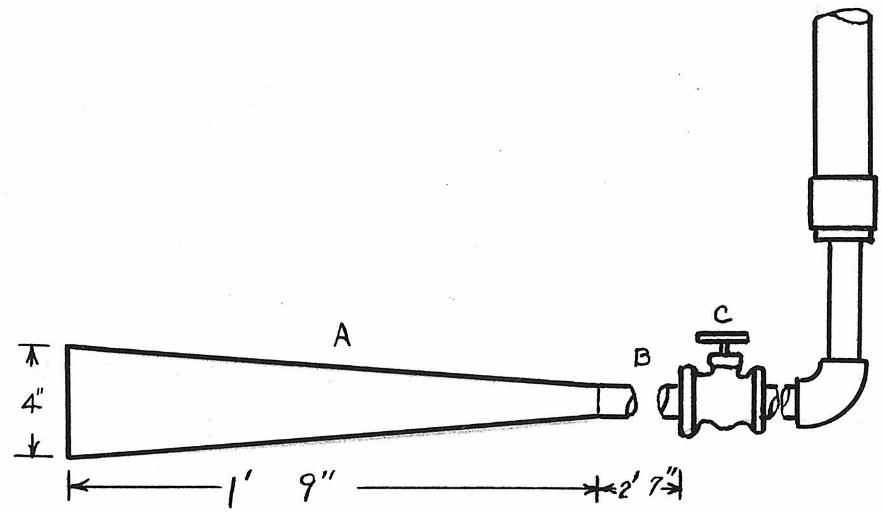

Fig 8a.

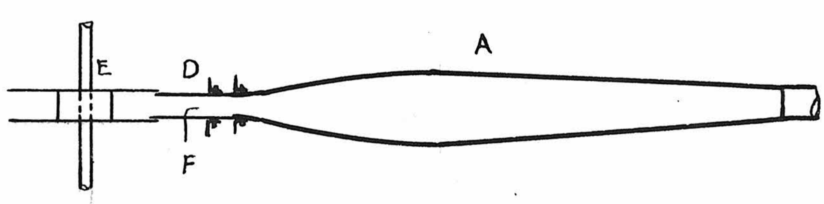

Fig 8b.

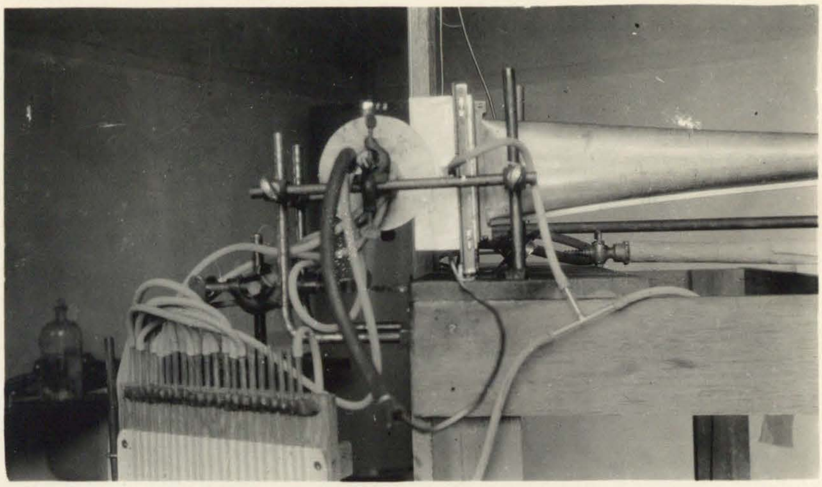

Fig. 9

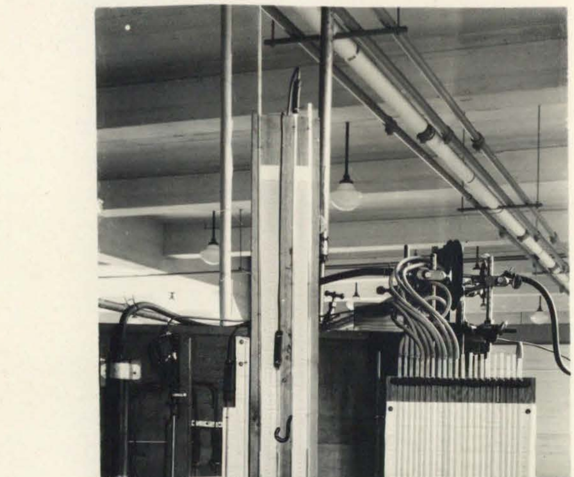

Fig. 10

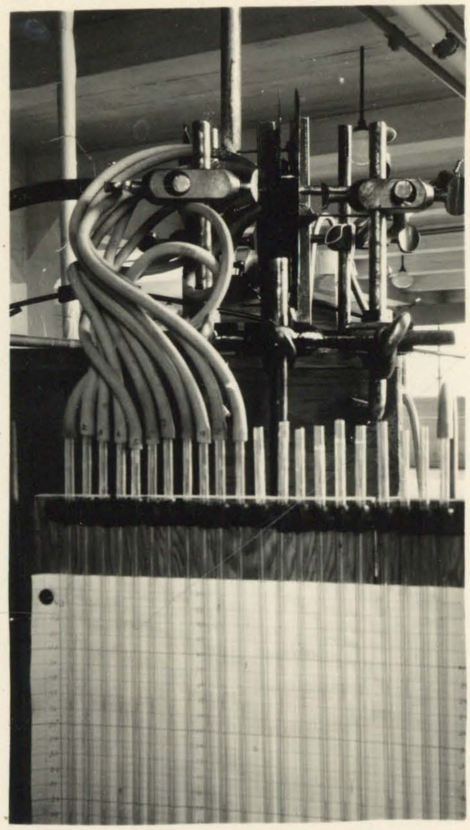

Fig. 11

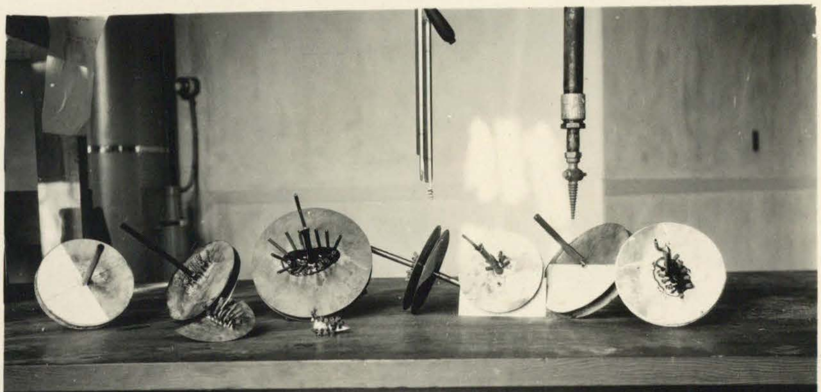

Fig. 12

differential water manometer at H , and the mercury manometers for measuring fluid meter pressure and nozzle pressure at J . The two closed tube mercury manometers also shown were not used.

Turbulence, which under the best of conditions was rather large, was reduced as much as possible by using a gate-valve C (Fig. 8), and placing it four and one-half feet from the test section. Convenience did not permit greater distance. In addition care was taken to avoid sharp angles at the connection between the expanding tube and the pipe B , and to keep the divergence of the tube gentle enough to avoid loss of contact between the walls and the stream.

3. The Fluid Meter

The fluid-meter is of the standard orifice type and was constructed according to specifications to make possible the use of tabulated orifice coefficients[15] and thus avoid calibration. These coefficients were later found to be unsuited and a more reliable set reported by a special research committee[16] on fluid-meters was adopted. The rate of flow is calculated by

$$W = C M \sqrt{2 g h \gamma_o \gamma}$$

where W = fluid flowing in pounds per second

h = pressure as measured on the differential water manometer in feet of water

γ_o = density of water in pounds per cubic foot

γ = density of air in pounds per cubic foot

M = fluid meter constant = $\frac{A}{\sqrt{R^4 - 1}}$ where

A is the cross-sectional area of the meter,

R is the ratio of diameter of meter to diameter of orifice, and

C is the orifice coefficient.

The constants are given in Table II. In the column headed W, i is the differential pressure in centimeters of water and P_f is the fluid meter pressure in cm. of mercury.

TABLE II.

Orifice Diameter in Inches	M	C	W
0.509	1.43×10^{-3}	0.659	$3.36 \times 10^{-4} \sqrt{i \times P_f}$
0.413	0.935×10^{-3}	0.639	$2.12 \times 10^{-4} \sqrt{i \times P_f}$

4. Experimental Procedure

The models were arranged for test as shown in Figures 9, 10, and 11. Two observers were required, one to control the air speed in the wind stream by the gate-valve and the other to read the manometers. For each model, pressure distributions were observed at various jet strengths and different negative angles of attack. In every case atmospheric pressure was used as the static pressure. From each set of manometer readings it was possible to compute the air speed of the stream, forces on the models, velocity of the jet, mass per second flowing from the nozzle, and the rate of expenditure of energy in the jet.

IV. Experimental Results

1. Test of Apparatus

Fig. 13 is a sample curve of the pressure distribution observed on the model airfoil of Göttingen 387-FB profile. After a comparison of such curves with the appropriate ones in Report No. 288 of the National Advisory Committee for Aeronautics, the apparatus was deemed satisfactory for the present work.

2. Forces From Pressure Distributions

It was desired to obtain from the observed pressure distribution the forces on the model parallel to the wind in one case and perpendicular to the wind in another. The first was obtained by plotting pressures in centimeters of alcohol as ordinates against the projection of the model upon a line perpendicular to the wind as abscissa; and the second, by again plotting pressures in centimeters of alcohol as ordinates but now against the projection of the model upon a line parallel to the wind as abscissa. The product of centimeters by millimeters representing the area under the curves was converted to force in pounds by multiplying by the factors

$$\text{cm} \times \text{mm} \times \rho_a \times 2.80 \times 10^{-4}$$

where ρ_a is the density of the alcohol in the multiple manometer.

The curves of pressure distribution are so numerous that only a few samples (Figs. 14 - 17) at zero angle of

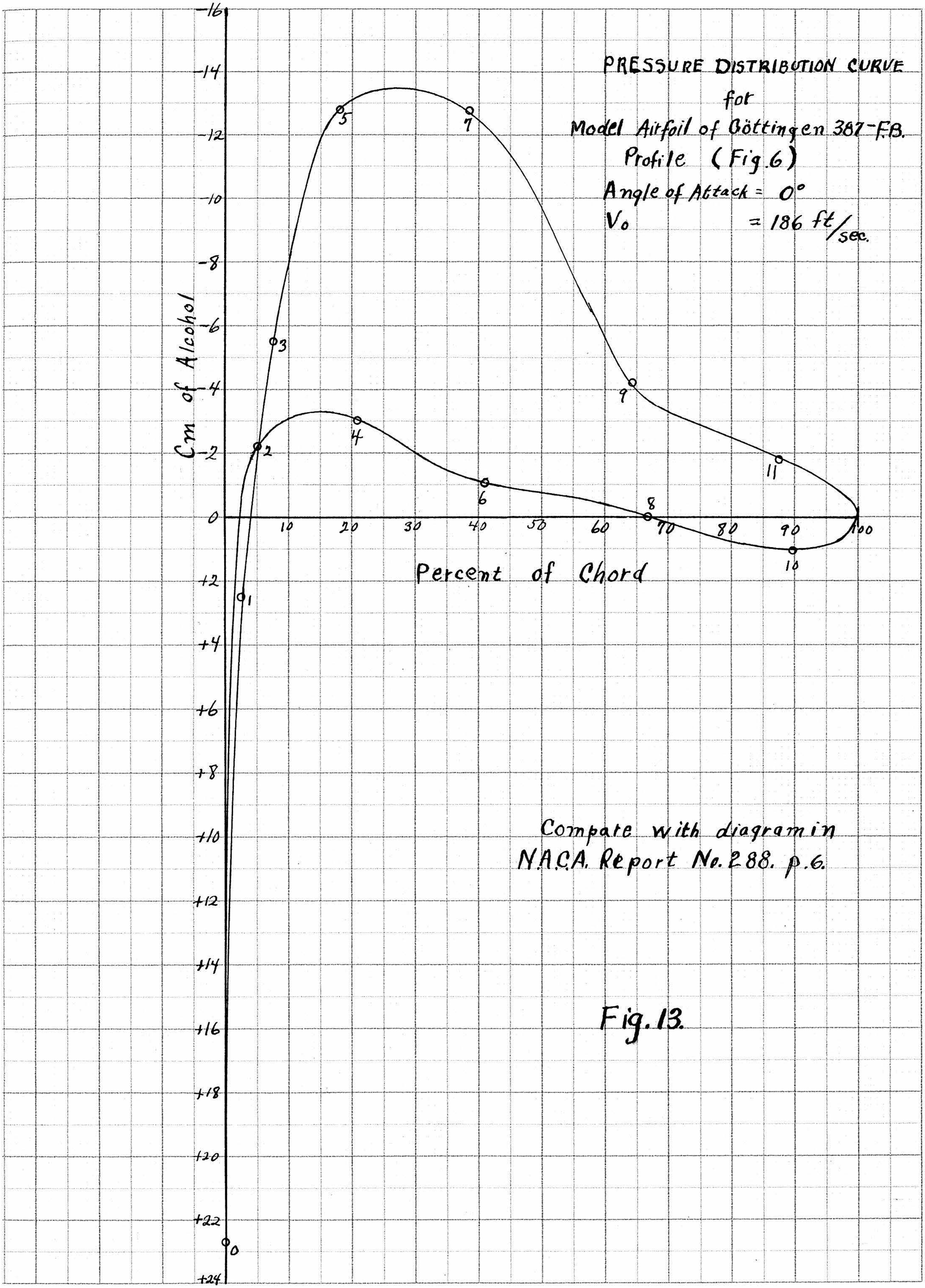
PRESSURE DISTRIBUTION CURVE
for
Model Airfoil of Göttingen 387-F.B.
Profile (Fig.6)
Angle of Attack = 0°
V₀ = 186 ft/sec.
Cm of Alcohol
Percent of Chord
Compare with diagram in
N.A.C.A. Report No. 288. p.6.

Fig. 13.

MODEL No 1

Pressure Distribution Curves for: Angle of Attack $= 0°$

W is wind pressure $V_0 = 158$ ft./sec.

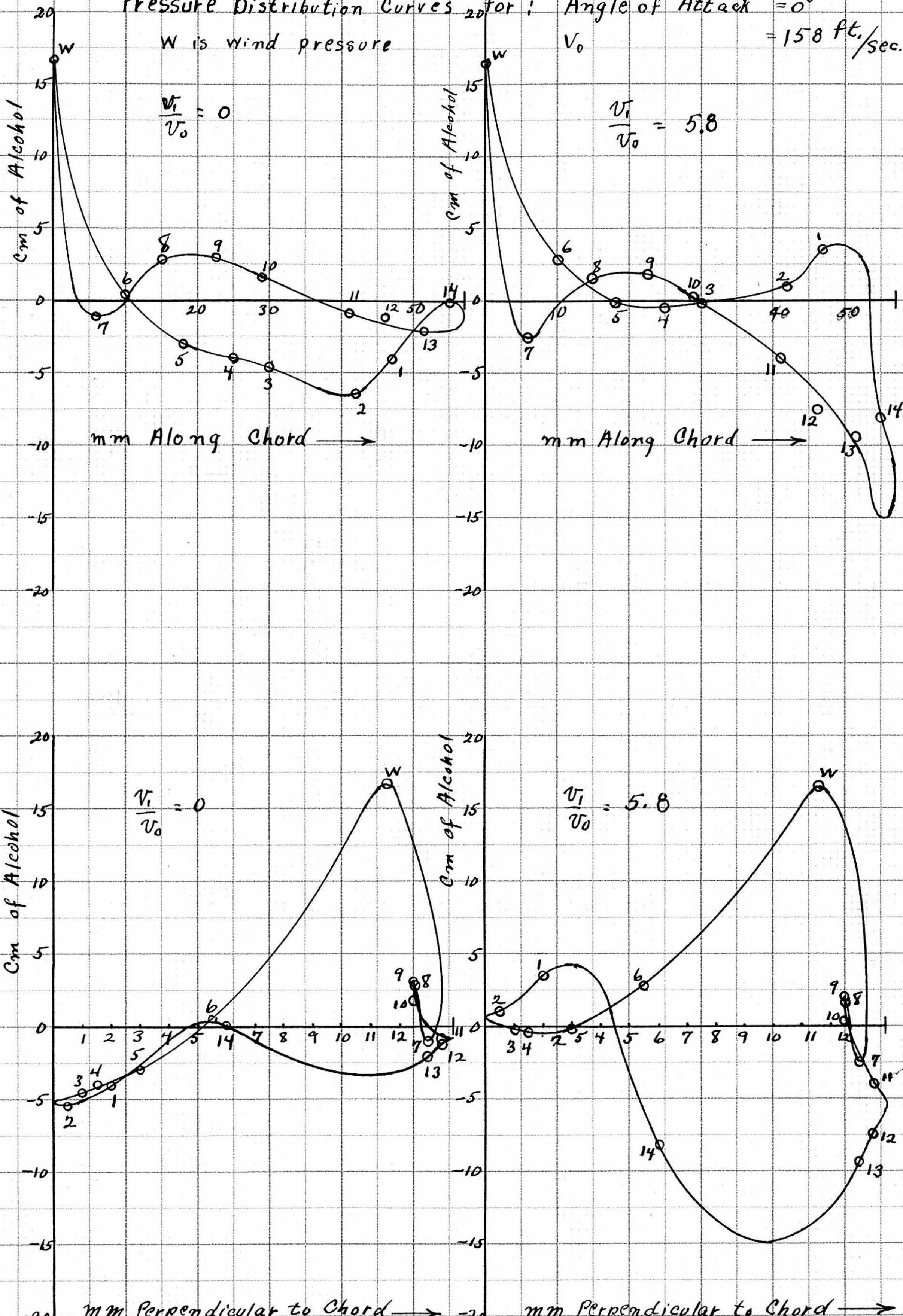

Fig. 14.

MODEL No 2

Pressure Distribution Curves for : Angle of Attack = 0°, V_0 = 158 ft/sec

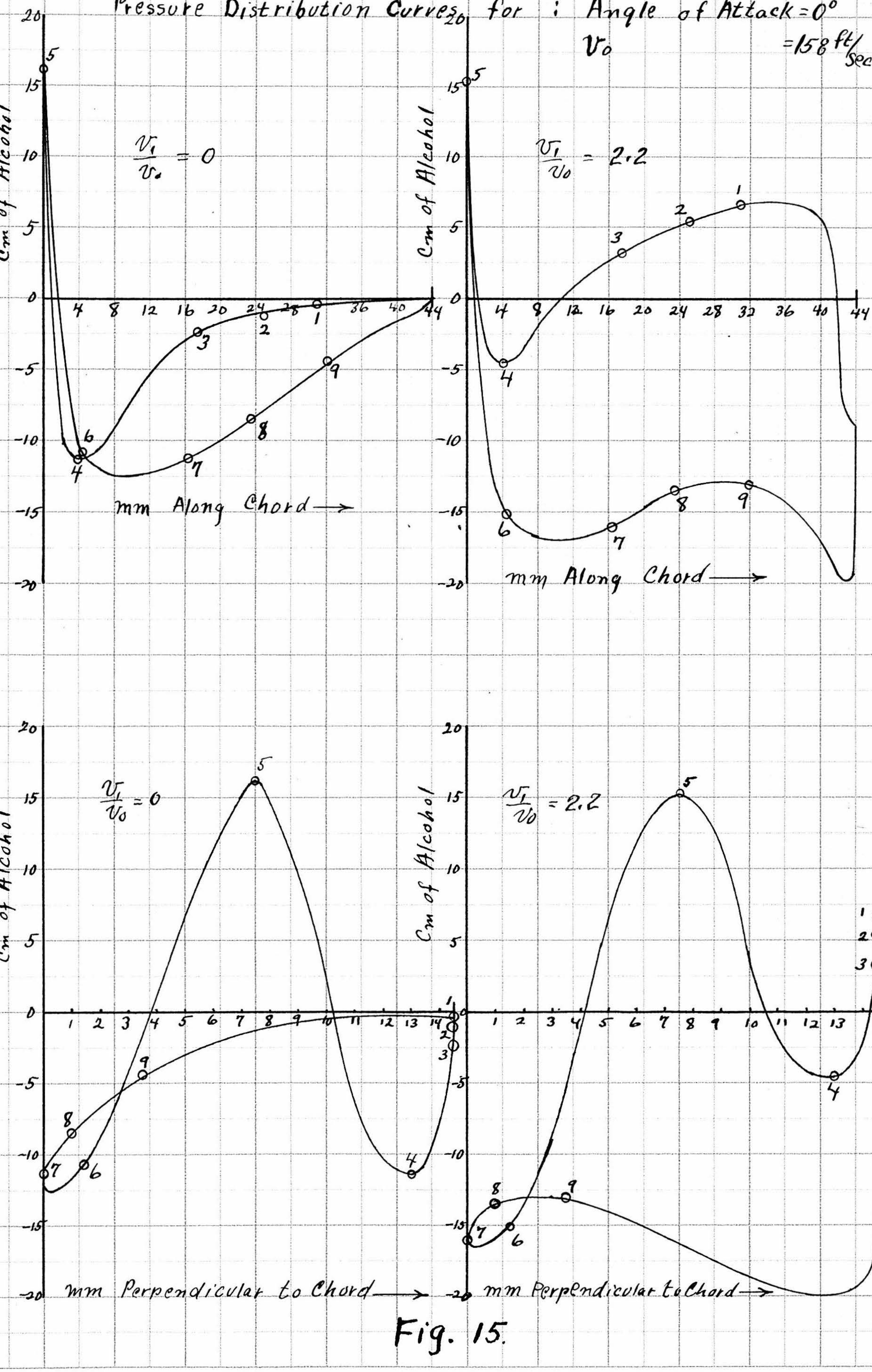

Fig. 15.

MODEL No 3.

Pressure Distribution Curves for: Angle of Attack = 0

W is wind pressure $\qquad v_0 = 158\ ft/sec$

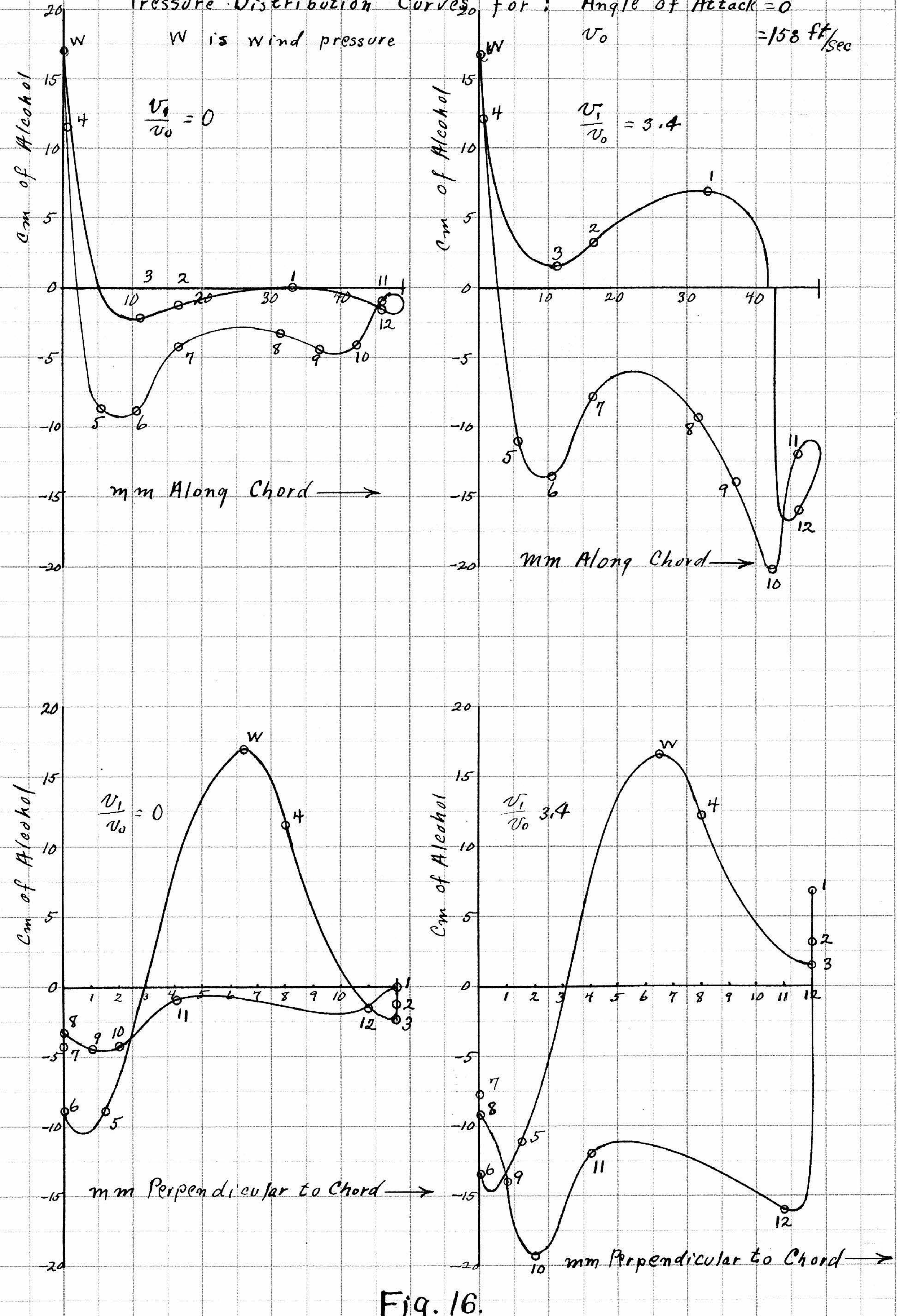

Fig. 16.

MODEL No. 4.

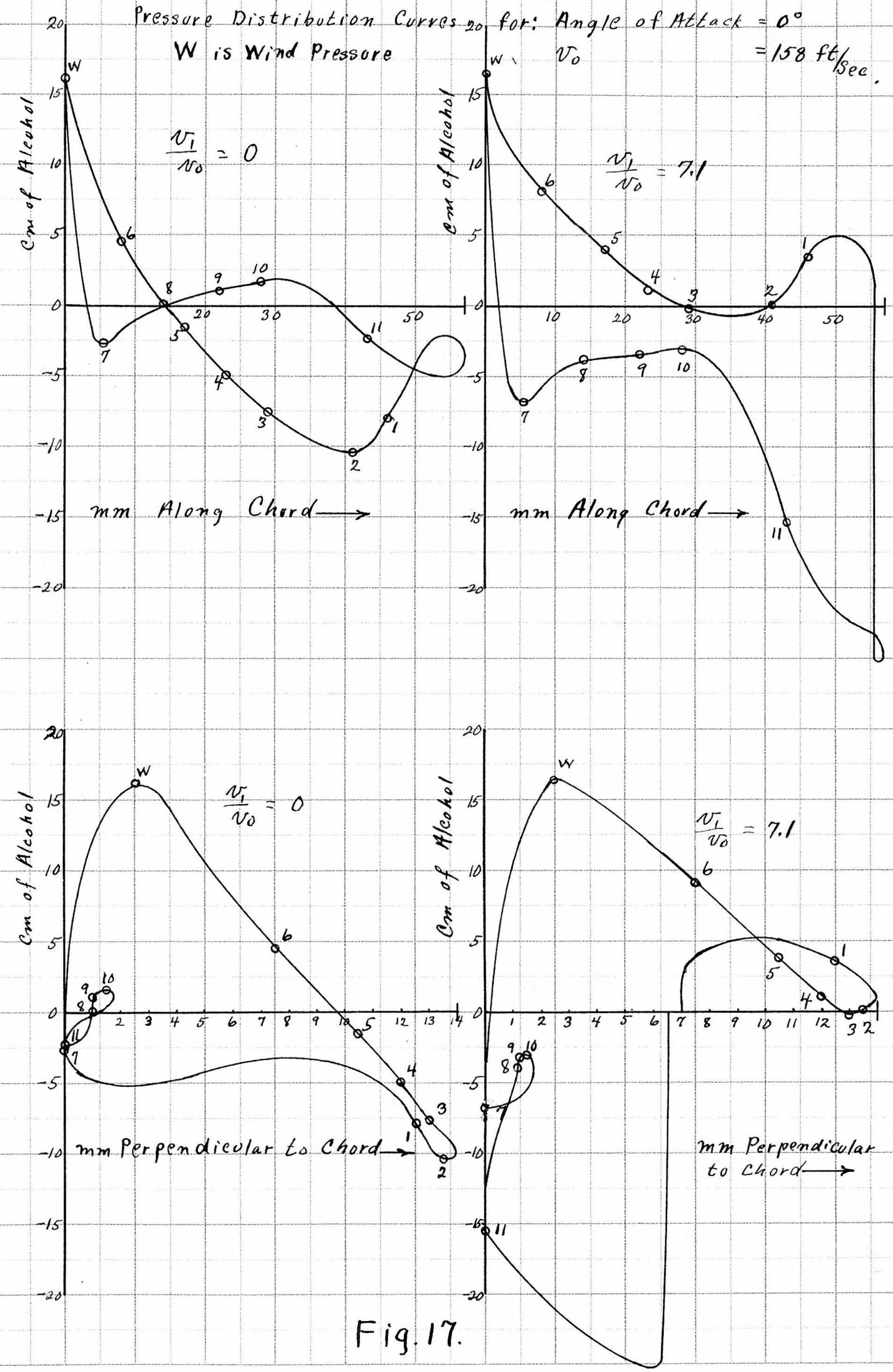

Fig. 17.

attack both with and without the jet are shown here. These typify the remainder of the curves for other angles of attack and jet strengths.

The total forces perpendicular and parallel to the wind are given in Table III under the headings F_{ty} and F_{tx} respectively. Adjacent columns marked F_y and F_x contain the difference in force with and without the jet. The variation of the forces with ratio of jet velocity to wind velocity is shown in Figures 18 - 21. Positive values means a lifting force and negative values sinking forces in the sense indicated by Figures 28 and 29.

The wind velocity was obtained from the dynamic pressure, q by the formula $q = 1/2\ \rho\ v_o^2$, where ρ is the density of the air and v_o is the velocity of the wind. The value of v_o was maintained at 158 ± 4 ft. per sec. for all the tests.

3. The Jet

Using the observed fluid meter pressure P_f and the drop in pressure i across the orifice in the formulas of Table II, the flow of air from the nozzle in pounds per second was obtained. The flows thus measured are plotted against absolute nozzle pressure in centimeters of mercury in Figures 22 - 25. On the same plots are shown the adiabatic flow curves computed by

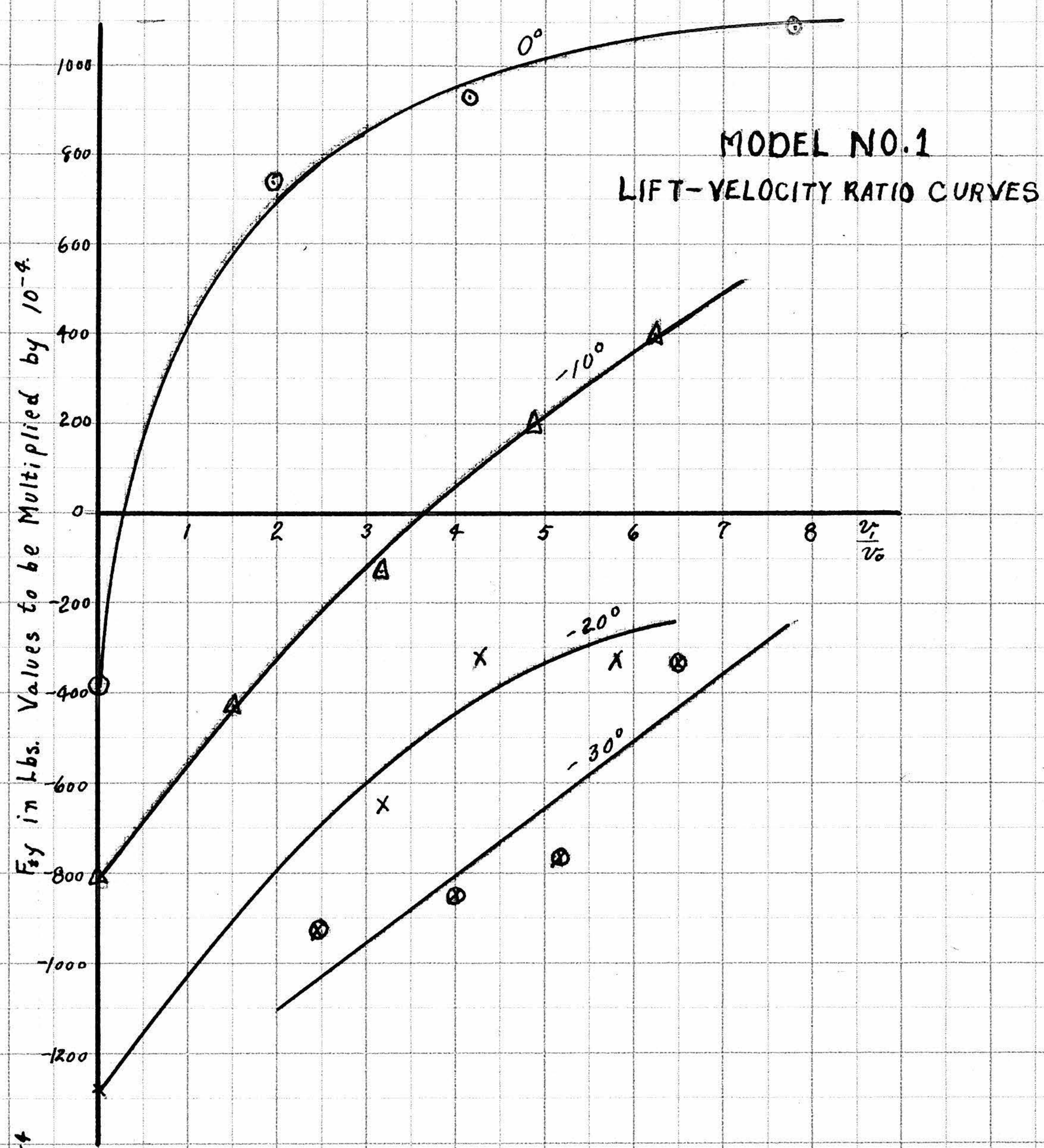
MODEL NO.1
LIFT-VELOCITY RATIO CURVES
0°
-10°
-20°
-30°
F_{ty} in Lbs. Values to be Multiplied by 10^{-4}.
1000
800
600
400
200
0
-200
-400
-600
-800
-1000
-1200
1
2
3
4
5
6
7
8
$\frac{v_1}{v_0}$

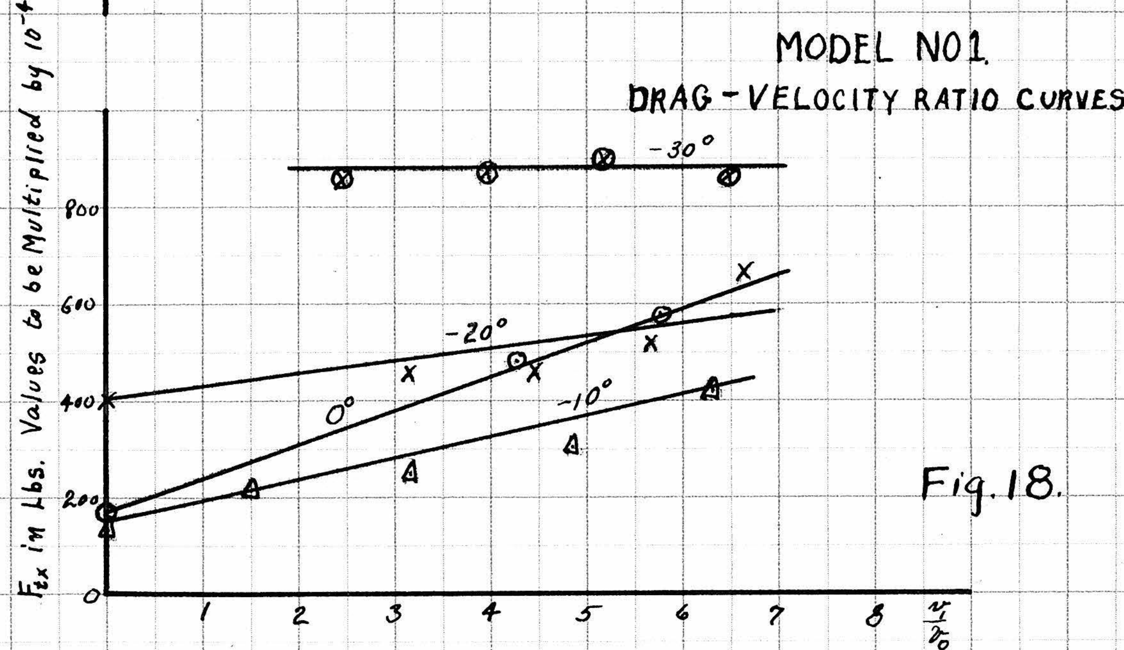
MODEL NO1.
DRAG-VELOCITY RATIO CURVES
-30°
-20°
0°
-10°
F_{tx} in Lbs. Values to be Multiplied by 10^{-4}
800
600
400
200
0
1
2
3
4
5
6
7
8
$\frac{v_1}{v_0}$

Fig. 18.

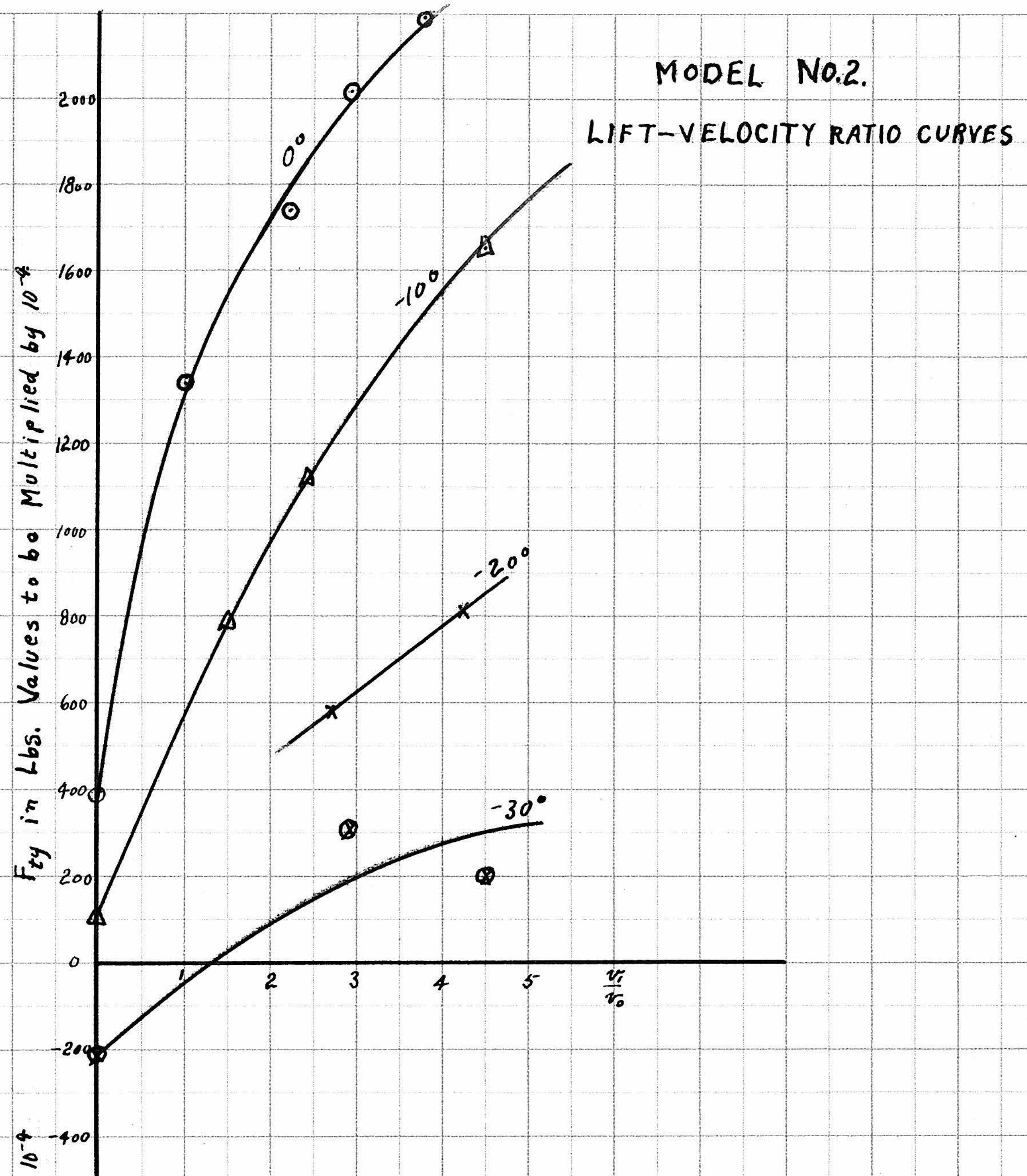
MODEL No.2.
LIFT-VELOCITY RATIO CURVES
F_{ty} in Lbs. Values to be Multiplied by 10^{-4}
0°
-10°
-20°
-30°
2000
1800
1600
1400
1200
1000
800
600
400
200
0
-200
-400
1
2
3
4
5
$\frac{v_1}{v_0}$

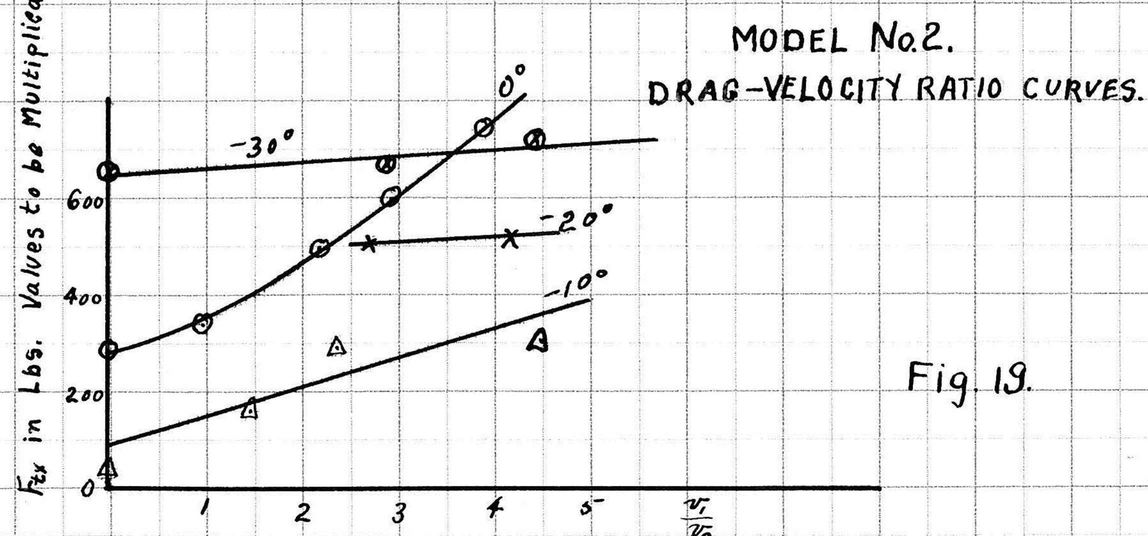
MODEL No.2.
DRAG-VELOCITY RATIO CURVES.
F_{tx} in Lbs. Values to be Multiplied by 10^{-4}
0°
-30°
-20°
-10°
600
400
200
0
1
2
3
4
5
$\frac{v_1}{v_0}$

Fig. 19.

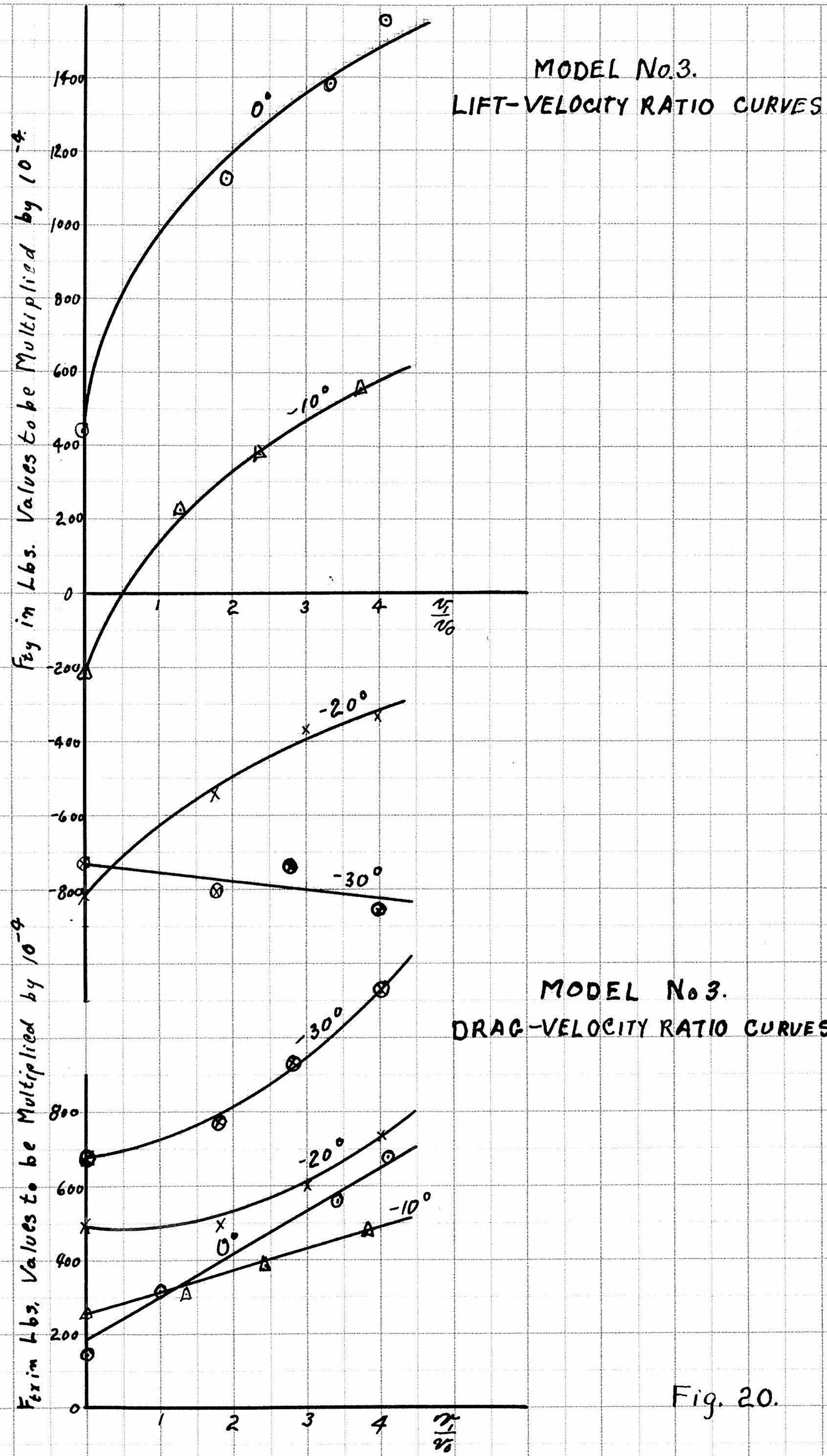

MODEL No.3.
LIFT-VELOCITY RATIO CURVES
Fzy in Lbs. Values to be Multiplied by 10^-4.
1400
1200
1000
800
600
400
200
0
-200
-400
-600
-800
0°
-10°
-20°
-30°
1
2
3
4
v1/v0
MODEL No 3.
DRAG-VELOCITY RATIO CURVES
Fzx in Lbs. Values to be Multiplied by 10^-4
800
600
400
200
0
-30°
-20°
-10°
0°
1
2
3
4
v1/v0

Fig. 20.

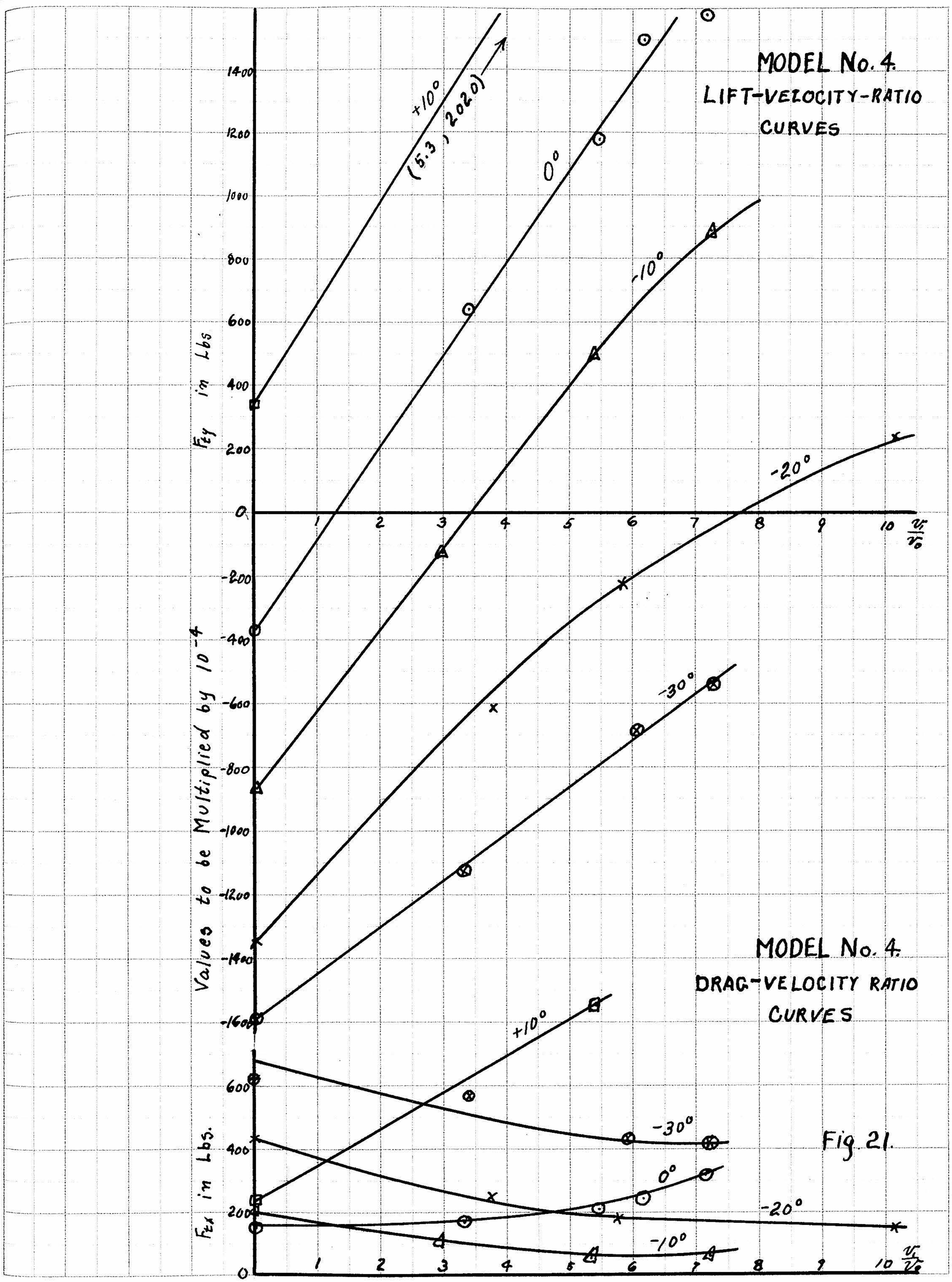
MODEL No. 4.
LIFT-VELOCITY-RATIO
CURVES
MODEL No. 4.
DRAG-VELOCITY RATIO
CURVES
F_{ty} in Lbs
Values to be Multiplied by 10^{-4}
F_{tx} in Lbs.
$\frac{V_r}{V_0}$
+10°
(5.3, 2020)
0°
-10°
-20°
-30°

Fig. 21.

MODEL No 1
NOZZLE FLOW - PRESSURE
CURVES

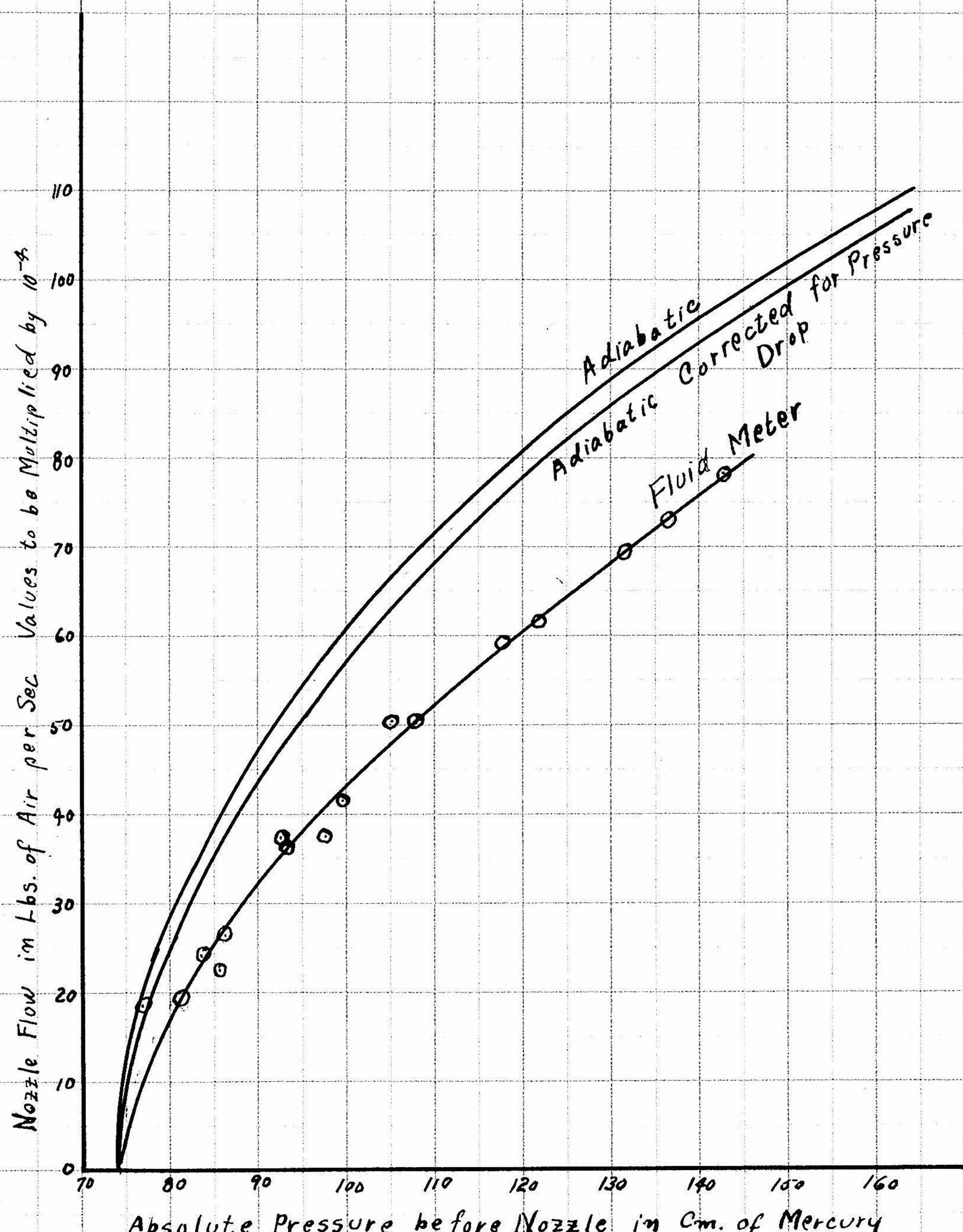

Fig. 22.

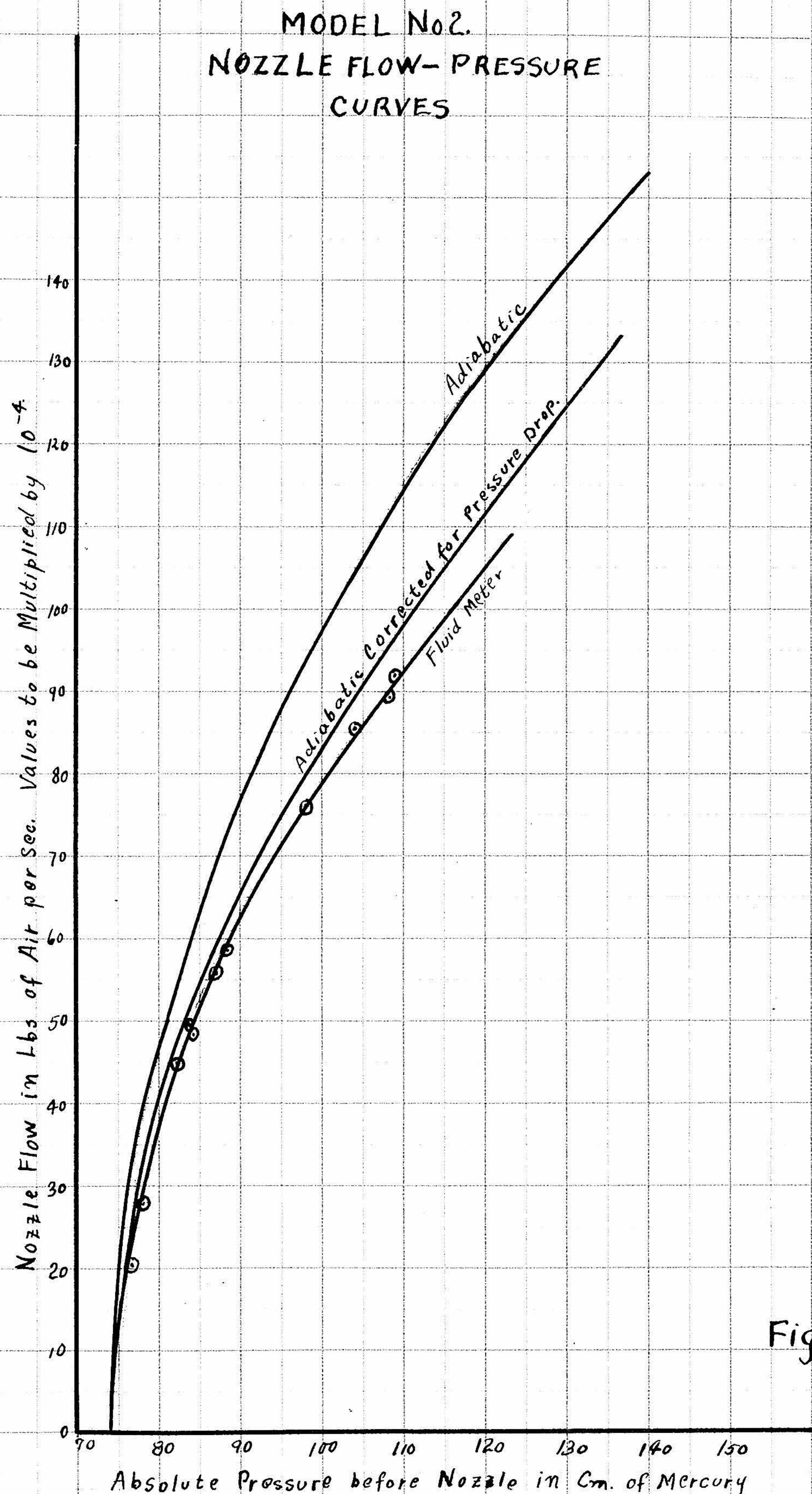

MODEL No2.
NOZZLE FLOW- PRESSURE
CURVES
Adiabatic
Adiabatic Corrected for Pressure Drop.
Fluid Meter
Nozzle Flow in Lbs of Air per Sec. Values to be Multiplied by 10^{-4}
Absolute Pressure before Nozzle in Cm. of Mercury
0
10
20
30
40
50
60
70
80
90
100
110
120
130
140
70
80
90
100
110
120
130
140
150

Fig. 23.

MODEL No. 3

NOZZLE FLOW - PRESSURE CURVES

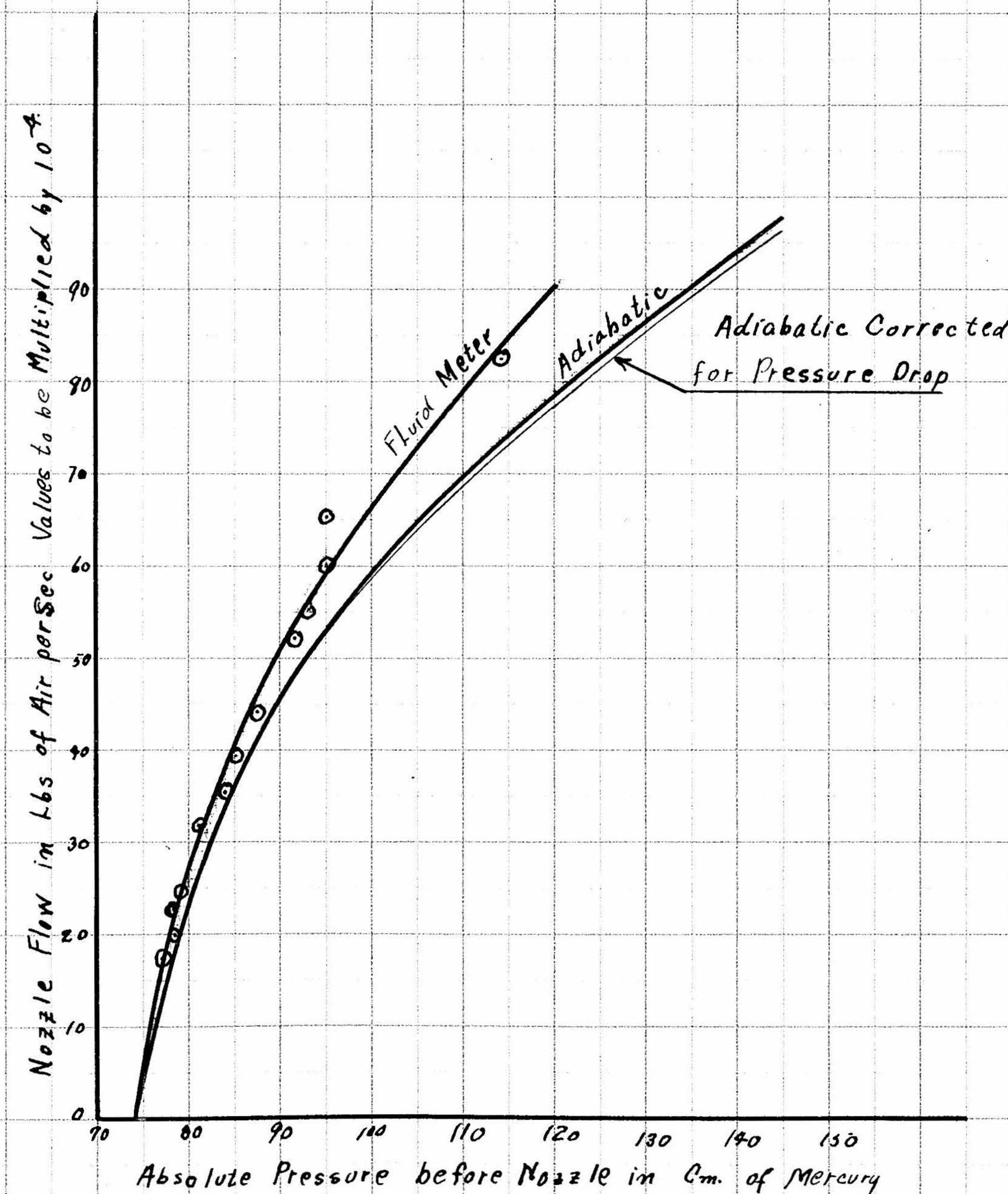

Fig. 24.

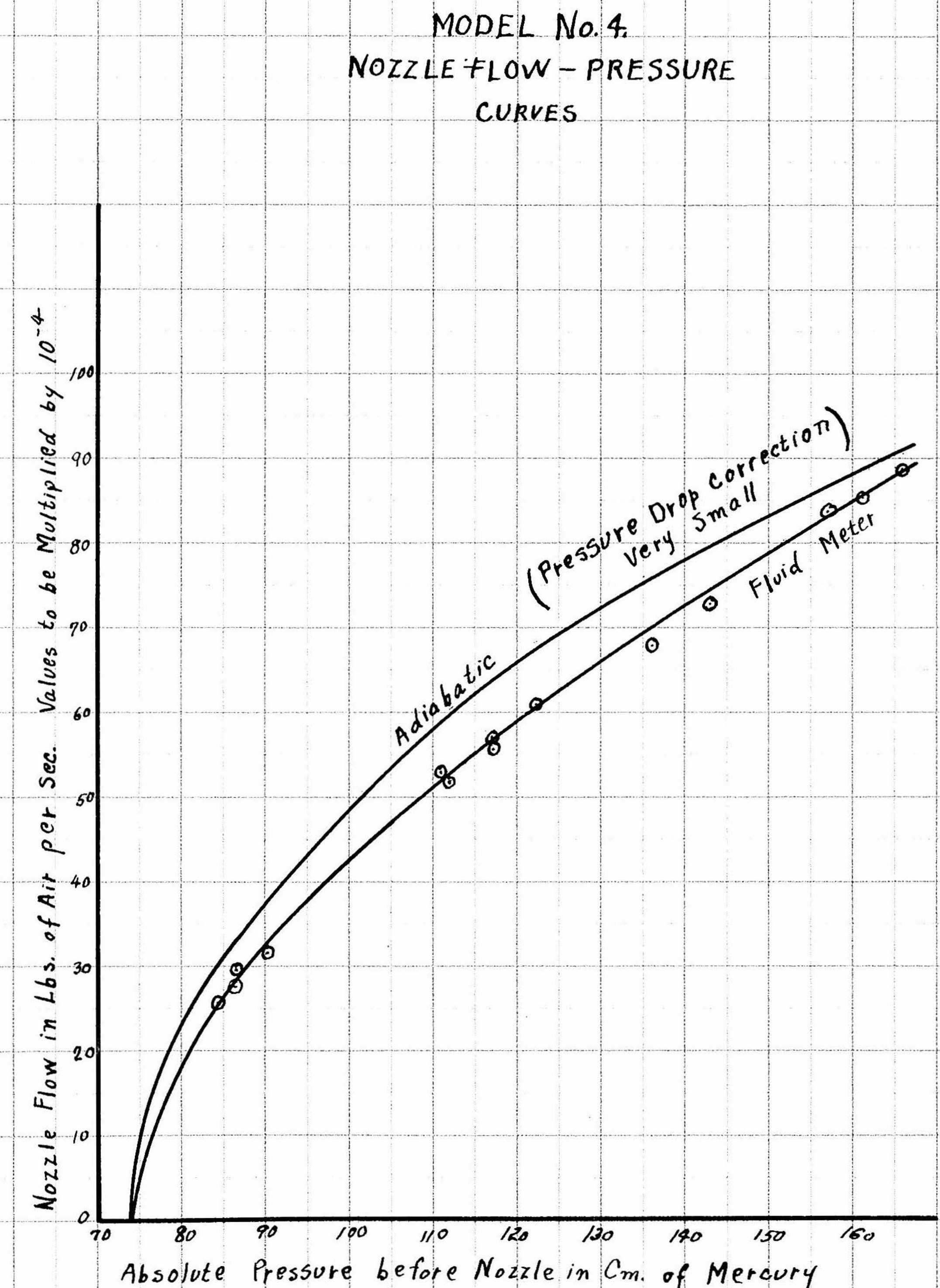

MODEL No. 4.
NOZZLE FLOW - PRESSURE
CURVES
Nozzle Flow in Lbs. of Air per Sec. Values to be Multiplied by 10^{-4}
Absolute Pressure before Nozzle in Cm. of Mercury
Adiabatic
(Pressure Drop Correction Very Small)
Fluid Meter
0
10
20
30
40
50
60
70
80
90
100
70
80
90
100
110
120
130
140
150
160

Fig. 25.

$$W = A\sqrt{\frac{2\,g\,k}{k-1}\,\frac{P_b^2}{RT_b}\left[\left(\frac{P_a}{P_b}\right)^{\frac{2}{k}} - \left(\frac{P_a}{P_b}\right)^{\frac{k+1}{k}}\right]} \qquad (4)$$

where W = flow in pounds per second

A = area of the orifice in square feet obtained from the orifice widths given in Table I

g = acceleration of gravity (32.2 ft. per sec.^{2})

k = ratio of specific heats (1.4 for air)

P_b = absolute nozzle pressure in pounds per square foot

P_a = average atmospheric pressure in the same unit as P_b

R = gas constant (53.35)

T_b = absolute temperature of the air Fahrenheit where the pressure is P_b (the average of 30°C converted to absolute Fahrenheit was used throughout)

The adiabatic flow curves marked "corrected" show the result of correcting for pressure drop along the channel from the point where nozzle pressures were measured to the orifice. The computations were made for the formula[17]

$$\Delta P_b = 1.41 \times 10^{-3}\, W^2 \ell \,\frac{C^5}{A_1^5}\,\frac{P_a}{P_b} \qquad (5)$$

where

ΔP_b = drop in pressure in pounds per square inch

W = flow in pounds per second as measured by the fluid meter

l = length of the channel in feet

C = perimeter of channel in inches

A_1 = average cross-section area in square inches

Due to the assumptions made about the nature of the surface the corrections are necessarily only approximate. The pressure loss will be used later in obtaining the correct jet velocity.

Considerable discrepancy between measured and adiabatic flows will be observed from the curves. The loss of pressure in every case except that for model No.3 brings the adiabatic values in better agreement with measured values, but the correction is too small to account for the total difference. Retardation of the jet due to impact with the exterior medium (Fig. 3) suggests itself as a possible explanation, but this effect also is too small, the maximum impact pressure being of the order of one centimeter of mercury under the conditions of the experiment. Measured values of the flow rather than the adiabatic are used in future calculations not only because of the foregoing uncertainties but also because the widths of the nozzle orifices were difficult to measure and may be slightly irregular.

The velocity v_1 of the jet in feet per second was calculated on the basis of adiabatic expansion by the formula

$$v_1 = \sqrt{2\, g\, \frac{k}{k-1}\, R\, T_b \left[1 - \left(\frac{P_a}{P_b}\right)^{\frac{k-1}{k}}\right]} \qquad (6)$$

where the quantities are the same as those in equation (4). As before the temperature of the jet varied but slightly and the average of 30°C. was used to determine T_b . Fig.26 obtained from equation (6) was used to determine all jet velocities.

In the case of model No. 2 where the pressure loss is large enough to take into account, velocities were determined from Fig. 26 by using for the pressure $P_b - \Delta P_b$. Such procedure is not strictly vigorous yet it is sufficiently accurate in view of the roughness of the pressure correction. For the other three models, velocity corrections were assumed to be unnecessary.

The reactive force F_1 of the jet in pounds was found by

$$F_1 = m_1 v_1$$

where $m_1 = \dfrac{\text{pounds of air flowing per second}}{g}$

These forces are plotted against P_b in Fig. 27.

The kinetic energy per second E_1 expended in the jet was obtained by substituting values of jet velocity taken from Fig. 26 (corrected in the case of Model No.2) and of values of the reactive force taken from Fig. 27 in the equation

$$E_1 = \frac{1}{2} F_1 v_1$$

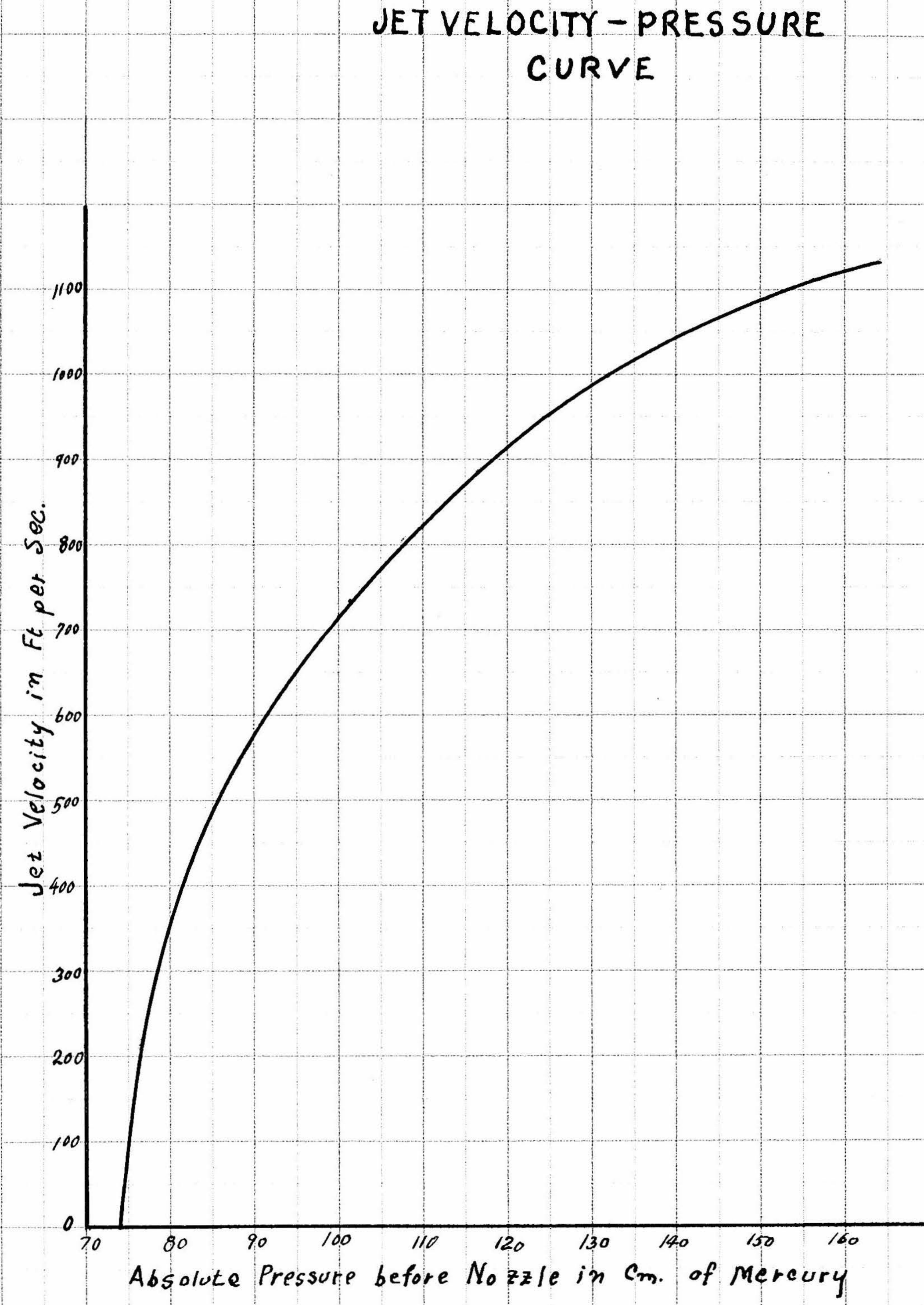
JET VELOCITY - PRESSURE
CURVE
Jet Velocity in Ft per Sec.
1100
1000
900
800
700
600
500
400
300
200
100
0
70
80
90
100
110
120
130
140
150
160
Absolute Pressure before Nozzle in Cm. of Mercury

Fig. 26.

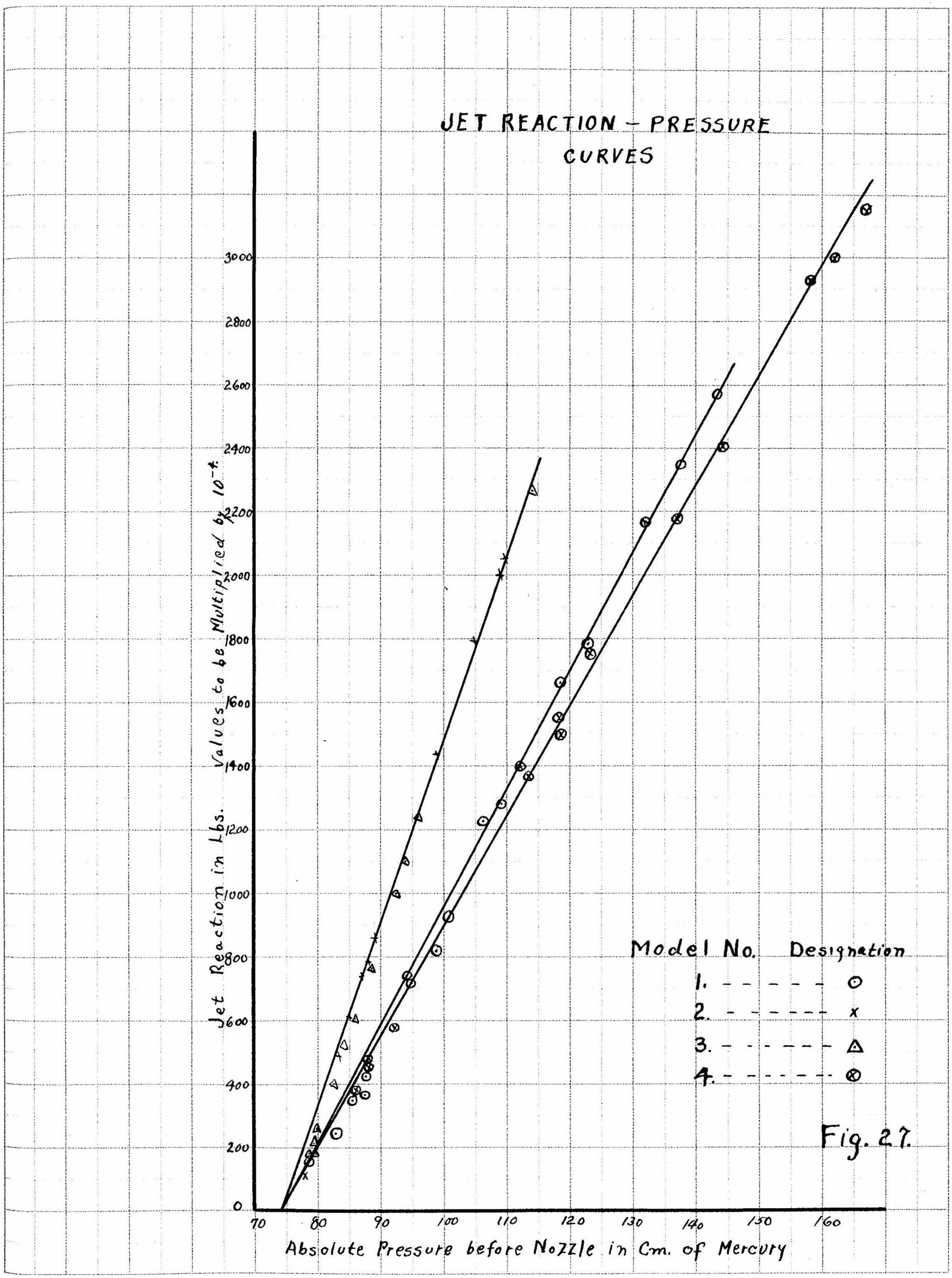
JET REACTION - PRESSURE
CURVES
Jet Reaction in Lbs. Values to be Multiplied by 10⁻⁴.
0
200
400
600
800
1000
1200
1400
1600
1800
2000
2200
2400
2600
2800
3000
70
80
90
100
110
120
130
140
150
160
Absolute Pressure before Nozzle in Cm. of Mercury
Model No. Designation
1. - - - - - ⊙
2. - - - - - x
3. - - - - - △
4. - - - - - ⊗
Fig. 27.

Figures 26 and 27 together with Table III contain the necessary quantities for determining propulsion efficiences and for making a comparison of the performance of the simple jet with that of the jet-foil.

TABLE III

Model No. 1

Angle of Attack	P_b in cm. of Mercury	Forces in lbs. derived from pressure on surface of model* F_{tx}	F_{ty}	F_x	F_y	E_1 in ft-lb per sec.
0	74.2	0.017	0.059	-	-	-
	83.6	0.036	0.054	-0.018	0.113	7.42
	99.5	0.047	0.072	-0.031	0.132	33.2
	117.4	0.053	0.087	-0.036	0.146	72.5
	142.2	0.069	0.100	-0.053	0.159	135.0
-10°	74.2	0.020	-0.103	-	-	-
	77.2	0.023	-0.061	-0.003	0.041	1.26
	86.0	0.027	-0.031	-0.007	0.072	11.0
	105.0	0.033	0	-0.013	0.103	44.3
	131.2	0.045	0.021	-0.025	0.123	107.0
-20°	74.2	0.043	-0.148	-	-	-
	85.7	0.048	-0.085	-0.005	0.064	10.3
	97.5	0.050	-0.051	-0.007	0.097	29.4
	121.5	0.058	-0.051	-0.018	0.097	82.2

* Figures 28 and 29

F_{tx} ..... (+) means a dragging force.

F_{ty} ..... (+) means a lifting force.
(-) means a sinking force.

F_x ..... (+) means a decrease in drag.
(-) means an increase in drag.

F_y ..... (+) means an increase in lift.
(-) means a decrease in lift.

TABLE III (Continued)

Model No. 2

Angle of Attack	P_b in cm. of Mercury	Forces in lbs. derived from * pressure on surface of model F_{tx}	F_{ty}	F_x	F_y	E_1** in ft-lb per sec.
0°	74.2	0.027	0.035	-	-	-
	76.2	0.031	0.130	-0.005	0.095	0.832
	81.7	0.049	0.170	-0.020	0.135	7.41
	86.7	0.057	0.199	-0.030	0.163	16.6
	97.7	0.071	0.218	-0.044	0.184	43.0
-10°	74.2	0.001	0.008	-	-	-
	77.6	0.014	0.075	-0.013	0.067	2.0
	83.5	0.027	0.109	-0.026	0.101	10.8
	107.8	0.028	0.162	-0.027	0.154	72.0
-30°	74.2	0.629	-0.025	-	-	-
	-	0.073	-0.026	-	-	-
	87.7	0.064	0.028	-0.001	0.053	18.6
	107.8	0.070	0.018	-0.007	0.043	72.0

* Figures 28 and 29

F_{tx} ..... (+) means a dragging force.

F_{ty} ..... (+) means a lifting force.
(-) means a sinking force.

F_x ..... (+) means a decrease in drag.
(-) means an increase in drag.

F_y ..... (+) means an increase in lift.
(-) means a decrease in lift.

** Corrected for pressure drop.

TABLE III (Continued)

Model No. 3

Angle of Attack	P_b in cm. of Mercury	Forces in lbs. derived from * pressure on surface of model F_{tx}	F_{ty}	F_x	F_y	E_1 in ft-lb per sec.
0	74.2	0.016	0.044	-	-	-
	78.7	0.032	0.112	-0.017	0.069	3.87
	87.2	0.047	0.137	-0.031	0.094	20.8
	94.7	0.068	0.154	-0.052	0.111	40.0
-10°	-	0.026	-0.022	-	-	-
	76.7	0.031	0.021	-0.005	0.043	1.3
	80.7	0.039	0.039	-0.012	0.061	7.0
	91.2	0.048	0.055	-0.022	0.076	30.8
-20°	-	0.051	-0.081	-	-	-
	77.7	0.050	-0.055	0.001	0.026	1.52
	84.6	0.061	-0.037	-0.010	0.044	14.6
	92.8	0.073	-0.034	-0.022	0.047	34.8
-30°	-	0.068	-0.073	-	-	-
	77.8	0.077	-0.082	-0.009	-0.008	1.85
	83.2	0.093	-0.075	-0.025	-0.001	13.6
	92.8	0.113	-0.088	-0.045	-0.013	60.5

* Figures 28 and 29

F_{tx} ..... (+) means a dragging force.

F_{ty} ..... (+) means a lifting force.
(-) means a sinking force.

F_x ..... (+) means a decrease in drag.
(-) means an increase in drag.

F_y ..... (+) means an increase in lift.
(-) means a decrease in lift.

TABLE III (Continued)

Model No. 4

Angle of Attack	P_b in cm. of Mercury	Forces in lbs. derived from * pressure on surface of model F_{tx}	F_{ty}	F_x	F_y	E_1 in ft-lb. per sec.
0°	74.2	0.034	-0.041	-	-	-
	86.2	0.035	0.061	-0.002	0.102	11.4
	112.0	0.040	0.114	-0.006	0.155	58.0
	136.0	0.043	0.148	-0.009	0.189	110.0
	157.0	0.050	0.156	-0.016	0.197	162.0
-10°	74.2	0.036	-0.089	-	-	-
	84.2	0.030	-0.015	0.006	0.074	8.5
	111.0	0.023	0.046	0.013	0.136	58.5
	161.0	0.025	0.087	0.011	0.177	168.0
-20°	74.2	0.060	-0.136	-	-	-
	90.5	0.044	-0.064	0.016	0.072	17.0
	117.0	0.036	-0.025	0.024	0.110	69.0
	143.0	0.033	0.020	0.027	0.156	127.
-30°	74.2	0.101	-0.16	-	-	-
	86.2	0.075	-0.115	0.025	0.046	12.1
	122.0	0.061	-0.071	0.039	0.090	80.9
	166.0	0.059	-0.056	0.042	0.105	179.0
+10°	74.2	0.042	0.033	-	-	-
	117.0	0.103	0.202	-0.061	0.169	63.0

* Figures 28 and 29

F_{tx} ...... (+) means a dragging force.

F_{ty} ...... (+) means a lifting force.
(-) means a sinking force.

F_x ...... (+) means a decrease in drag.
(-) means an increase in drag.

F_y ...... (+) means an increase in lift.
(-) means a decrease in lift.

4. Energy Relations and Efficiency

We now come to the most important part of the experimental problem, namely, a quantitative determination of the value of the jet-foil scheme. The preceding data are interesting in that they show what effect the jet has upon the lift and drag of the models and also show some relation between this effect and the strength of the jet, but as yet the important question of propulsive efficiency is unanswered. To reach our goal it is highly important to determine propulsive efficiency and particularly to compare the simple jet and the jet-foil in this respect; but at the sametime this is perhaps the most difficult task yet undertaken. The problem is a complex one requiring a thorough analysis of conditions of air flow about the models and the changes produced in them by the jet. Unless this is done the method of attack is likely to be wrong and lead to much misinformation.

We have at our disposal at least three ways of attacking the problem of propulsive efficiency, each one of which deals with the jet in a different light. These are: first, a comparison of the efficiency with which the simple jet in one case and the jet plus the jet-foil in another accelerate a given stream of air from rest; second, a determination of the over-all efficiency of the jet-foil as a propelling device compared again to the simple jet; and third, to find how well the jet-foil has performed its one function, namely, the conversion of the left-over kinetic energy of the jet into useful work. We shall consider each of these in detail with a view to using all of them if possible, and if not of choosing the best from among them.

The first illustrates best the advantages of the jet-foil over the simple jet, for it is here that the efficiency of the simple jet is a minimum. However, this method involves the rather artificial procedure of selecting a certain fraction of the jet from which the jet-foil derives its forces and then comparing the efficiency of this fraction, used by itself to set up motion normal to the air stream, with its efficiency when used for the same purpose in conjunction with the jet-foil.

The second, while certainly an indication of the practical worth of the jet-foil is objectionable here, first because it is unfair due to the poor aerodynamic qualities of the models, and second because it combines the efficiency of the simple jet and the jet-foil leaving their separate contributions unknown. The unfairness of the test arises from the fact that the profile drag of the models, which in the present case is large, is a matter of design, and if given sufficient attention may be reduced to little more than that of skin friction. For this reason it may be stated as approximately true that the question of the drag of the models is not a part of the question of transverse jet action.

The third type of treatment lends itself to the elimination of the drag of the models and in addition differentiates between the effect of the jet and that of the jet-foil. The pressure distribution method of determining forces is particularly adapted to the present method since the reaction of the jet and the forces resulting from pressures on the surface of the model are known separately. Considering the drawbacks to the first and second methods and the advantages of the third, together with the fact that no more illuminating information can be obtained than that concerning the effectiveness of the jet-foil in making use of the jet disturbance in the surrounding air, it would seem advisable to concentrate our attention here and examine the characteristics of the jet-foil from this one viewpoint only. This we shall do, but first we must examine some of the assumptions which must necessarily be made about the air flow.

All available methods must be based upon changes in the velocity of the wind stream. This requires that the velocity distribution of the stream be either known or assumed. We must be satisfied here with an assumption, and the one which we shall make is that the velocity of the stream is uniform and that changes which are produced affect the entire stream alike. This we know is not strictly true, yet since the stream is small we may assume as a fair approximation that the circulation effects are transmitted to all parts of the stream uniformly. The effect of a nonuniform distribution is to decrease the mass term and increase the velocity term in the kinetic energy equation $1/2\ m\ v^2$ and cause the actual energy involved to be greater than the calculated amount. The failure of the assumption will cause calculated efficiencies to be too low.

A second assumption, made for the sake of simplicity, is that the mass of air added to the stream by the jet is negligible compared to the mass of the stream itself. Any error made here will tend to compensate for that introduced by a loss of part of the stream. We are thus not likely to add any uncertainty by neglecting the mass of the jet in the receding stream.

Having chosen the method of attack and having partially examined its worth, we are prepared now to use the available data to make the necessary computations.

Calling F_{ox} the drag of the model without the jet and F_{oy} its lift, we obtain the lift F_y and drag F_x resulting from the jet alone by

$$F_y = F_{ty} - F_{oy}$$

$$F_x = F_{tx} - F_{ox}$$

It is now necessary to closely examine the flow in the rear of the model to see just what effect the jet has here.

All of the models have rather blunt trailing edges. We thus infer that without the jet the flow does not follow around the sharp curvature of the trailing edge at all, and that there exists in the rear of the model a wake of eddying air. When the jet acts we see the drawing process illustrated by Fig. 5 to be removing this eddying mass of air by causing it to follow the rear surface of the jet.

Considering the action in detail we find three effects. First and most obvious, kinetic energy is added to the air. Second, the pressure is reduced in the rear of the model producing an increase in drag over the trailing edge surface and an over-all increase in drag unless compensation is made elsewhere. The result is a deflection of the stream. Third, the partial or total removal of the wake makes it possible for the flow to better follow around the sharp curvature of the trailing edge, bringing about either a reduction in the initial drag of the model or an exchange of its eddy making drag for one giving rise to stream deflection.

All three effects contribute to F_y since all three give rise to velocity components normal to the streams. However, in calculating energy addition, we are interested only in the portion of F_y resulting from the first. The force F_y is measured in its totality and can be corrected for the purpose of energy computation by the force arising from the second and third effects. Here we meet difficulty, for we have only F_x to use in making the correction. Since F_{ox} was assumed constant to obtain F_x, we recognize the necessity for the assumption that the third effect is absent altogether. Such an assumption may be of questionable validity, but it must be made unless we wish to forego the elimination of the effect of the model. The method of making the correction will be taken up later.

We have concentrated on the trailing edge since this is the only place about the model that the jet action may reduce the turbulent drag. The forces with which we are working have arisen from every part of the model.

In order to know what effect jet action has upon the stream we must know how the model itself changes the magnitude and direction of the stream velocity. For this purpose we take the X-direction as that of the unaltered stream; then calling the deflected stream s and its components of velocity v_{sx} and v_{sy}, we may write

$$v_{sy} = \frac{F_{oy}}{M}$$

and

$$v_o - v_{sx} = \frac{F_{ox}}{M}$$

where F_{oy} and F_{ox} are the lift and drag respectively upon the model without the jet, M is the mass per second of the stream, and v_o is its initial velocity. Solving for v_{sx} we have

$$v_{sx} = v_o - \frac{F_{ox}}{M}$$

The angular deflection ϕ of the stream is then given by

$$\tan \phi = \frac{F_{sy}}{v_{sx}} = \frac{F_{oy}}{v_o M - F_{ox}}$$

and the velocity v_s of the altered stream by

$$v_s = \sqrt{v_{sx}^2 + v_{sy}^2}$$

The forces F_x and F_y, together with the jet reaction F_1, are next resolved normal and parallel to the stream s. The components are illustrated by Fig. 29. They are summarized here as follows:

	Normal	Parallel
F_x	F_{xn}	F_{xp}
F_y	F_{yn}	F_{yp}
F_1	F_{1n}	F_{1p}
Algebraic sum	F_{tn}	F_{tp}

A velocity v_n normal to the stream s results from normal forces, and is given by

$$v_n = \frac{F_{tn}}{M}$$

The change in v_s produced by parallel forces may be found by means of the force equation

$$F_{tp} + M\, v_s = M\, v_{st}$$

where v_{st} is the final velocity component parallel to the stream s under the action of parallel forces. If the change in v_s is Δv_s, we have

$$\Delta v_s = v_{st} - v_s = \frac{F_{tp}}{M}$$

Having determined the velocities in the direction of the force components, we are in position to determine the power added to the stream by the separate forces. The total added power is the sum of the amount contributed by the forces individually. For this purpose we make use of two relations:

FORCE DIAGRAMS

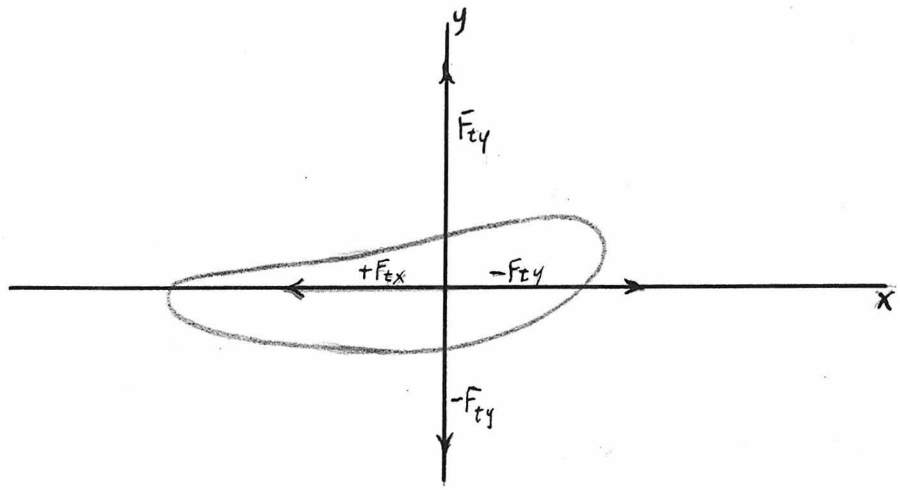

Fig 28 TOTAL FORCES

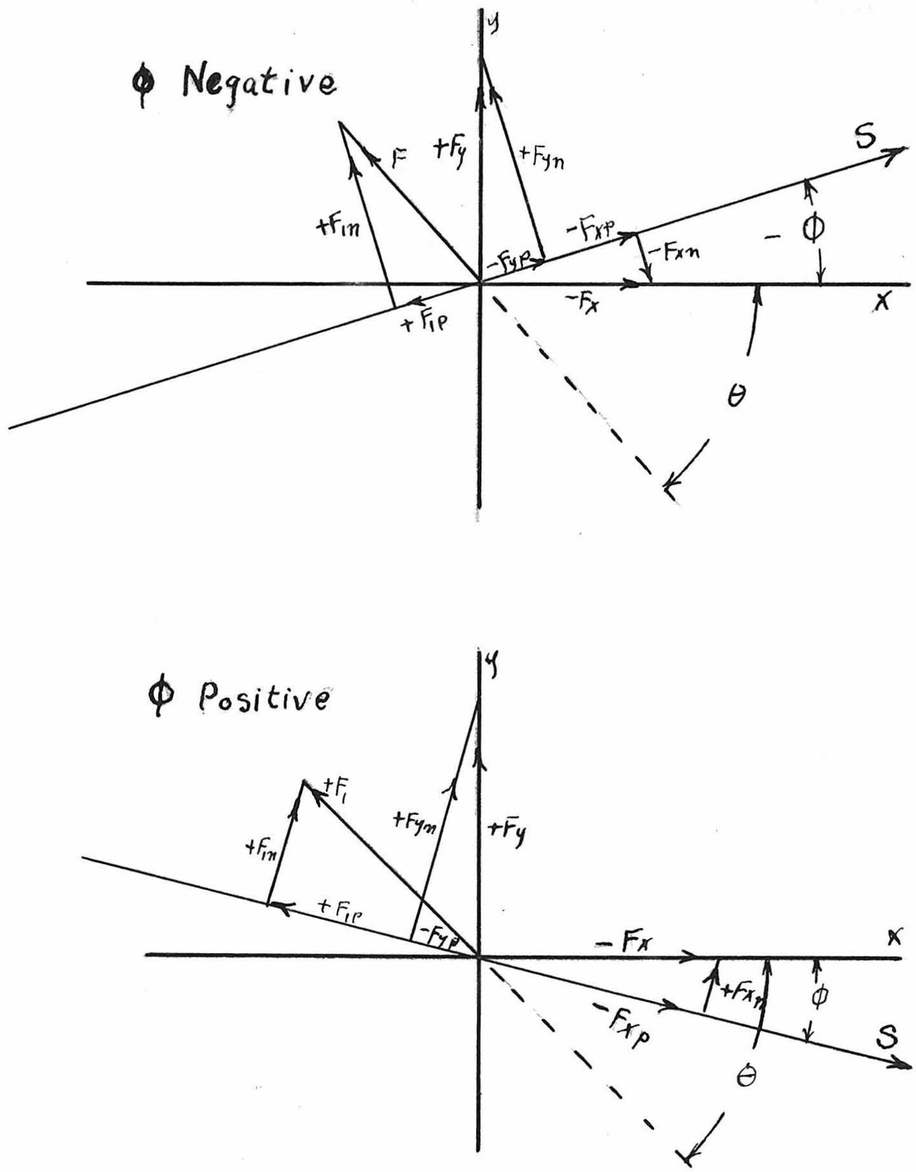

Fig. 29 DIFFERENCE OF FORCES

$$\text{Power} = \text{Force} \times \text{Velocity}$$

when the velocity is constant, and

$$\text{Power} = 1/2 \text{ Force} \times \text{Velocity}$$

when velocity is the result of the forces.

We have mentioned previously that forces normal to the stream, which in the present case are F_{yn} and F_{xn}, may arise from two sources, one from an addition of power to the stream and the other from a deflection of the stream. The former we shall call F'_η and the latter F''_η. We then have

$$(F_{xn} + F_{yn}) = F'_\eta + F''_\eta$$

Where $(F_{px} + F_{py})$ is known and has a negative sign, in other words is a drag, we may determine F''_η and thus obtain F'_η alone to compute correctly the added power. The correction need be made only when $(F_{px} + F_{py})$ is negative, that is, when the jet has increased the drag.

We eliminate F''_η as follows: The stream is retarded by an amount given by

$$\delta v_s = \frac{F_{px} + F_{py}}{M}$$

The remaining velocity is then: $v_s - \delta v_s$

Since we assume that the retardation results in a deflection, we have

$$v_s^2 = v_n'^2 + (v_s - \delta v_s)^2$$

and solving for v'_n

$$v'_n = \sqrt{v_s^2 - (v_s - \delta v_s)^2}$$

where v_n' is the component normal to the stream s resulting from a deflection rather than an addition of power.

The force F_η'' has produced v_n' and hence may be found from

$$F_\eta'' = v_n' M$$

We thus obtain for the power adding normal force

$$F_n' = (F_{xn} + F_{yn}) - F_n''$$

This correction is so great that in most cases where the jet causes an increase in the drag the calculated power absorbed by the jet-foil is zero or negative. This would seem to indicate that the jet added no power to the stream, which condition seems very doubtful in view of the strong disturbing action of the jet. A better explanation on the basis of turbulence will be given after the results have been presented. Since it is of interest to see the effect of assuming the entire normal velocity to be due to power addition by the jet, a set of results will be included where the correction for the drag has not been made.

The power added to the stream by the jet reaction F_1 is

$$E_j = F_{1p} v_s + 1/2 F_{1p} \Delta v_s + 1/2 F_{1n} v_n$$

and that added by forces on the model is

$$E_{fc} = v_s(F_{xp}+F_{yp}) + 1/2 \Delta v_s (F_{xp}+F_{yp}) + 1/2 v_n (F_{yn}+F_{xn})$$

when jet action has decreased the drag.

When the jet has increased the drag, which was the case for all the models except No.4, the added power is found by

$$E_{fc} = 1/2\ v_n\ F_n'$$

If we neglect the correction of normal forces, the power added is

$$E_f = 1/2\ v_n\ (F_{yn} + F_{xn})$$

The difference between E_j and E_1 of Table III is the power which goes into the disturbance in the surrounding air and is available for absorption by the jet-foil. How completely the jet-foil does the absorbing may be expressed in percentage by

$$\eta_{fc} = \frac{E_{fc}}{E_1 - E_j} \times 100 \qquad (7)$$

where the normal forces are corrected if necessary. In the absence of correction, we have

$$\eta_f = \frac{E_f}{E_1 - E_j} \times 100 \qquad (8)$$

Table IV contains values of efficiency calculated by equations (7) and (8) for each model at various angles of attack and a variety of jet strengths. In the same table will be found a comparison between the jet reaction and the forces on the model arising from the action of the jet upon the surrounding air.

TABLE IV

Model No. 1

Angle of Attack	$\frac{V_1}{V_o}$	η_{fc} *	η_f	$F_1 \times 10^2$	$\sqrt{F_x^2 + F_y^2} \times 10^2$
0	2.8	0	32	3.30	11.3
	4.5	0	11	9.30	13.2
	5.7	0	7	16.1	14.6
	6.7	0	5	25.6	15.9
-10°	1.5	0	49	1.05	4.14
	3.2	0	10	4.30	7.21
	4.9	0	6	11.4	10.3
	6.3	0	4	21.5	12.3
-20°	3.2	0	9	4.1	6.39
	4.3	0	7	8.60	9.73
	5.9	0	4	17.7	9.73

Model No. 2

Angle of Attack	$\frac{V_1}{V_o}$	η_{fc} *	η_f	$F_1 \times 10^2$	$\sqrt{F_x^2 + F_y^2} \times 10^2$
0	1.0	0	over 100	1.04	9.50
	2.2	0	71	4.30	13.6
	2.8	0	43	7.40	16.6
	3.9	0	22	14.1	18.8
-10°	1.5	0	26	1.70	6.85
	2.4	0	15	5.60	10.5
	4.5	0	8	20.2	15.6
-30°	2.9	0.2	6	8.00	5.25
	4.5	0	2	20.2	4.30

*Zero efficiency means that the jet-foil has absorbed no power.

TABLE IV (Continued)

Model No. 3

Angle of Attack	$\frac{v_1}{v_o}$	η_{fc}*	η_f	$F_1 x 10^2$	$\sqrt{F_x^2 + F_y^2} + 10^2$
0	2.0	0	19	2.50	7.03
	3.4	0	9	7.80	9.64
	4.1	0	7	12.3	12.2
-10°	1.3	0	27	1.30	4.25
	2.4	0	10	3.75	6.23
	3.8	0	4	10.2	7.96
-20°	1.8	0	15	1.80	2.64
	3.0	0	4	6.10	4.48
	4.0	0	2	11.1	5.25
-30°	1.3	0	0	1.80	1.30
	3.2	0	0	5.40	2.50
	6.9	0	0	11.1	4.65

Model No. 4

0	3.3	3	21	4.10	10.2
	5.4	0.5	9	13.3	15.5
	6.1	0.5	8	2.2	18.9
	7.1	0	6	29.2	19.7
-10°	2.9	4	17	3.5	7.43
	5.3	4	7	13.0	13.6
	7.2	2	5	30.6	17.7
-20°	3.7	5	8	5.70	7.21
	5.7	8	4	15.0	11.2
	6.7	0.5	5	24.2	15.6
-30°	3.2	38	38	4.3	5.22
	5.9	8	8	16.8	9.80
	7.2	4	4	32.4	11.3
+10°	5.3	0	10	15.0	18.0

*Zero efficiency means that the jet-foil has absorbed no power.

V. Discussion of Results

Considering the assumptions which were made concerning the nature of the air flow, we can regard the computed efficiencies as little more than a rough indication of the effectiveness of the jet-foil as an absorber of kinetic energy. We can at least put Model No.4 in a class by itself as definitely showing the effect for which we are searching.

Figures 18 - 21 show that the jet gives rise to forces normal to the wind on the jet-foil which are in all cases, except that for Model No.3, at -30° angle of attack, favorable to positive efficiencies. If we compute the energies on the basis of normal forces only, there is little difference in the performance of the models. All show decreasing efficiency with increasing jet strength, and generally lower efficiencies for larger negative angles of attack. However, when we take into account the dragging forces arising from the jet, conditions appear quite different. Here the efficiency of Models No.1, No.2, and No.3 reduce to zero throughout, while that of No.4 is somewhat lowered, but still retains a value which we can trust is high enough to be outside of experimental error in indicating an efficiency other than zero.

The increasing drag may easily be explained by the lowering of pressure around the trailing edge of the jet-foil, but it is difficult to understand why this drag did not result in a proportionate increase in lift. The only logical explanation is that the drag is not a stream deflecting type. In other words, jet action has increased the amount of turbulence when it should have decreased it by partially destroying the turbulent wake of the model. If we examine the profiles in Fig. 6 and compare the nozzle locations of Models No.1, No.2, and No.3 with that of No.4, we find a possible answer. Where the flow must be drawn around the trailing edge and back along the under surface, as it must be with the first three, we would expect not only poor drawing action, but also a large amount of turbulence in the resulting motion. This condition has largely been remedied in Model No.4.

VI. Conclusions

The results of Table IV appear rather discouraging to one who is looking to the jet-foil for more efficient jet propulsion. The highest corrected efficiency η_{fc} given in Table IV would not justify a practical consideration of the scheme.

However, when we look again at the aerodynamical theory, we are forced to conclude that a jet-foil designed for smooth flow around the trailing edge would appear to be capable of yielding very high efficiencies. The design of better jet-foils must be directed toward improving trailing edge conditions. For practical application, the nozzle must be radically changed, both to accommodate hot gases and to overcome the mechanical disadvantages of a long narrow slit. With the necessary alterations, if these are possible, and improvements in design, the jet-foil scheme has prospects of becoming of practical value. Much work remains to be done upon these two phases of development as well as upon the untouched problems relating to heat engine efficiency.

The writer wishes to express his thanks to Dr. C. B. Millikan and Dr. A. L. Klein for the helpful suggestions which they have given regarding the experimental technique, and for their aid in finding publications relating to the problem, and to Dr. H. Bateman for pointing out certain characteristics of the two-dimensional jet and of the cylindrical jet of hot gas. In addition the writer wishes to thank Dr. H. L. Dryden of the Bureau of Standards for suggesting a number of important references and for criticizing the writer's views on the action of viscosity in determining jet form.

References

1. Edgar Buckingham: Jet propulsion for Airplanes. National Advisory Committee for Aeronautics, Report No. 159.

2. Lanchester: Aerodynamics, p. 79.

3. Lamb: Hydrodynamics, p. 98, 5th ed.; and Bassett, A.B.: Treatise on Hydrodynamics, p. 120, Vol. 1.

4. Lanchester: Aerodynamics, p. 134.

5. Lanchester: Aerodynamics, p. 135.

6. Dorsey, N.E.: The Flow of Liquid Through Capillaries, Phys. Rev., pp. 833-845, Vol. 28, No.4, Oct., 1926.

7. Smoluchowski, M.M.: Sur la formation des veines d'efflux dans les liquides, Bull. de L'Acad. de Cracovie, 1904.

8. Lanchester: Aerodynamics, p.137.

9. Prandtl, L.: Bericht über Untersuchungen zur ausgebildeten Turbulenz, diese Zeitschrift, p. 136, Vol. 5, 1925.

10. Tollmien, Walter: Zeitschrift für Angewandte Mathematik und Mechanik, p. 468, Vol. 6, 1926.

11. Lamb: Hydrodynamics, p. 16, 5th ed.

12. Rabouchinsky, M.D.: Sur la resistance des fluides et la réaction d'un jet; Congres International de la Navigation Aerinne, p. 177, Vol. 2.

13. Montgomery Knight and Oscar Loeser, Jr.: Pressure Distribution over a Rectangular Monoplane Wing Model up to 90° Angle of Attack. National Advisory Committee for Aeronautics, Report No. 288.

14. Henke, Paul E.: Influence of the Orifice on Measured Pressures. National Advisory Committee for Aeronautics, Technical Notes, Report No. 250.

15. Harris: Compressed Air, pp. 35, 139.

16. Fluid Meters. Their Theory and Application. Part 1. Report of A.S.M.E. Special Research Committee on Fluid Meters, pp. 36-37, 2nd ed.

17. Luke: Engineering Thermodynamics, p. 1118.